

EUMETSAT Satellite Application Facility on Climate Monitoring

The EUMETSAT
Network of
Satellite Application
Facilities



Validation Report SSM/I products HOAPS release 3.2

Near Surface Specific Humidity	CM-141 (NSH_HOAPS)
Near Surface Wind Speed	CM-142 (SWS_HOAPS)
Latent Heat Flux	CM-143 (LHF_HOAPS)
Precipitation	CM-144 (PRE_HOAPS)
Evaporation	CM-145 (EVA_HOAPS)
Freshwater Flux	CM-146 (EMP_HOAPS)

Reference Number:



SAF/CM/DWD/VAL/HOAPS

Issue/Revision Index:

1.1

Date:

25.03.2011

 	EUMETSAT SAF on CLIMATE MONITORING Validation Report HOAPS release 3.2	Doc.No.:SAF/CM/DWD/VAL/HOAPS Issue: 1.1 Date: 25.03.2011
---	---	--

Document Signature Table

	Name	Function	Signature	Date
Author	Axel Andersson	HOAPS Team scientist		12/11/2010
Author	Karsten Fennig Marc Schröder	CM SAF scientist		25/03/2011
Editor	Rainer Hollmann	Science Coordinator		25/03/2011
Approval	Rainer Hollmann	Science Coordinator		25/03/2011
Release	Martin Werscheck	Project Manager		

Distribution List

Internal Distribution	
Name	No. Copies
DWD Archive	1
CM SAF Team	1

External Distribution		
Company	Name	No. Copies
PUBLIC		1

Document Change Record

Issue/Revision	Date	DCN No.	Changed Pages/Paragraphs
1.0	12/11/2010	SAF/CM/DWD/VAL/HOAPS/1	First official version.
1.1	18/03/2011	SAF/CM/DWD/VAL/HOAPS/1.1	Changes DRI-4




 	EUMETSAT SAF on CLIMATE MONITORING Validation Report HOAPS release 3.2	Doc.No.:SAF/CM/DWD/VAL/HOAPS Issue: 1.1 Date: 25.03.2011
---	---	--

Table of Contents

List of Figures	4
List of Tables	5
1 Executive Summary	6
1.1 Applicable documents	7
1.2 Reference Documents	7
2 The EUMETSAT SAF on Climate Monitoring	8
3 Introduction	8
4 Data Sets for Comparison with HOAPS	10
4.1 IFREMER Satellite Derived Turbulent Fluxes V3	10
4.2 NOCS v2.0	10
4.3 GPCP V2	10
4.4 TRMM 3B43	11
4.5 ERA-Interim	11
5 Evaluation of HOAPS Parameters	11
5.1 Methodology	11
5.2 Near surface specific humidity	11
5.3 Near surface wind speed	14
5.4 Evaporation and Latent heat flux	17
5.5 Precipitation	21
5.6 Freshwater Flux	24
6 Decadal stability	27
7 Conclusions	29
8 References	31

List of Figures

Figure 1: Climatological mean field (left) and zonal mean annual cycle (right) of HOAPS near surface specific humidity q_{air} for the years 1988–2005.	12
Figure 2: Difference of the 1992-2005 climate mean HOAPS near surface specific humidity and ERA interim (upper left), NOCS v2.0 (upper right), and IFREMER Flux (lower right). The lower left panel shows the global monthly mean humidity time series of each data set and the zonal mean humidity for the overlapping time period 1992-2005.	13
Figure 3: Climatological mean field (left) and zonal mean annual cycle (right) of HOAPS near surface wind speed for the years 1988–2005.	14
Figure 4: Difference of the 1992–2005 climate mean HOAPS wind speed and ERA-Interim (upper left), NOCS v2.0 (upper right), and IFREMER flux (lower right). The global monthly mean wind speed time series of each dataset (lower-left, top). and the zonal mean wind speed (lower-left, bottom) for the overlapping time period 1992–2005.	15
Figure 5: Climatological mean field (left) and zonal mean annual cycle (right) of HOAPS evaporation for the years 1988–2005.....	17
Figure 6: Difference of the 1992–2005 climate mean HOAPS evaporation and ERA-Interim (upper left), NOCS v2.0 (upper right), and IFREMER flux (lower right). The global monthly mean evaporation time series of each dataset (lower-left, top). and the zonal mean evaporation (lower-left, bottom) for the overlapping time period 1992–2005.	18
Figure 7: Climatological mean field (left) and zonal mean annual cycle (right) of HOAPS precipitation for the years 1988–2005.....	21
Figure 8: Difference of the 1992–2005 climate mean HOAPS precipitation and (upper left) ERA-Interim, (upper right) TRMM 3B43 (1998–2005), and (lower right) GPCP V2. The lower-left panel shows the global monthly mean precipitation time series of each dataset and the zonal mean precipitation for the overlapping time period 1992–2005 (1998–2005 for TRMM 3B43).....	22
Figure 9: Climatological mean field (left) and zonal mean annual cycle (right) of HOAPS freshwater flux for the years 1988–2005.....	25
Figure 10: Difference of the 1992–2005 climate mean HOAPS freshwater flux and (upper left) ERA-Interim, (upper right) IFREMER–GPCP, and (lower right) IFREMER–GPCP minus ERA-Interim. The lower-left panel shows the global monthly mean freshwater flux time series of each dataset and the zonal mean freshwater for the overlapping time period 1992–2005.	26
Figure 11: Time series of global monthly mean anomalies of HOAPS parameters minus reference (thin black line) for the time period 1988-2005. The thick black lines are 5-monthly running means. The light grey (dark	

	EUMETSAT SAF on CLIMATE MONITORING Validation Report HOAPS release 3.2	Doc.No.:SAF/CM/DWD/VAL/HOAPS Issue: 1.1 Date: 25.03.2011
---	---	--

grey) shaded areas represent the threshold (target). The dotted lines are the target bias requirements for the global mean values. The red line shows the estimated linear trend and the green line is the no-trend line. 28

List of Tables

Table 1: Requirements for near surface humidity product CM-141 as given in the PRD [RD 1] Accuracy numbers are given for global mean values. Regional larger deviations may occur..... 13



Table 2: Requirements for near surface wind speed product CM-142 as given in the PRD [RD 1]. Accuracy numbers are given for global mean values. Regional larger deviations may occur..... 16

Table 3: Requirements for evaporation (CM-143) and latent heat flux (CM-145) products as given in the PRD [RD 1]. Accuracy numbers are given for global mean values. Regional larger deviations may occur. 20

Table 4: Requirements for precipitation product CM-144 as given in the PRD [RD 1]. Accuracy numbers are given for global mean values. Regional larger deviations may occur..... 23

Table 5: Requirements for freshwater flux product CM-146 as given in the PRD [RD 1]. Accuracy numbers are given for global mean values. Regional larger deviations may occur..... 26

Table 6: Results from the decadal stability analysis of global monthly mean anomalies (number are per decade)..... 27

 	EUMETSAT SAF on CLIMATE MONITORING Validation Report HOAPS release 3.2	Doc.No.:SAF/CM/DWD/VAL/HOAPS Issue: 1.1 Date: 25.03.2011
---	---	--

1 Executive Summary

This CM SAF report provides information on the validation of the CM SAF HOAPS release 3.2 data sets derived from Special Sensor Microwave/Imager (SSM/I) observations onboard Defence Meteorological Satellite Program (DMSP) platforms F08, F10, F11, F13, F14 and F15. The same algorithm has already been used in the Hamburg Ocean-Atmosphere Parameters and fluxes from Satellite (HOAPS, <http://www.hoaps.org/>) data set (Andersson et al. 2010).

Today, latent heat flux and precipitation over the global ocean surface can be determined from microwave satellite data as a basis for estimating the related fields of the ocean surface freshwater flux. HOAPS - the Hamburg Ocean Atmosphere Parameters and fluxes from Satellite data – is the only generally available satellite based data set with consistently derived global fields of both evaporation and precipitation and hence of freshwater flux for the period 1987 to 2008.

This report presents an evaluation of

Near surface specific humidity [CM-141, NSH_HOAPS],

Wind speed at 10m height [CM-142, SWS_HOAPS],

Latent heat flux at sea surface [CM-143, LHF_HOAPS],

Precipitation [CM-144, PRE_HOAPS],

Evaporation [CM-145, EVA_HOAPS],



Freshwater flux [CM-146, EMP_HOAPS],

from the HOAPS data set against recently available reference data sets from reanalysis and other satellite observation projects as well as in-situ ship measurements and largely follows Andersson et al. (2010).

The CM SAF HOAPS 3.2 release is a so called heritage release, which means that no changes are made to any of the physical retrievals. The main difference between both releases is an updated version of the satellite inter-calibration procedure. However, as the reference satellite for the relative calibration remains unchanged, the mean brightness temperature differences are smaller than 0.5 K and the derived physical parameters will not change significantly.

Results show, that the general climatological patterns are reproduced by all data sets. Global mean time series agree within about 10 % of the individual products, while locally larger deviations may be found for all parameters. HOAPS often agrees better with the other satellite derived data sets than with the in-situ or the reanalysis data. The agreement usually improves in regions of good in-situ sampling statistics. The biggest deviations of the evaporation parameter result from differences in the near surface humidity estimates. The precipitation data sets exhibit large differences in highly variable regimes with the largest absolute differences in the ITCZ and the largest relative differences in the extra-tropical storm track regions.

The resulting freshwater flux estimates exhibit distinct differences in terms of global averages as well as regional biases. Compared to long term mean global river runoff data, the ocean surface freshwater balance is not closed by any of the compared fields. The data sets exhibit a positive bias in E-P of 0.2 mm/d to 0.5 mm/d, which is in the order of 10 % of the evaporation and precipitation estimates.

 	EUMETSAT SAF on CLIMATE MONITORING Validation Report HOAPS release 3.2	Doc.No.: SAF/CM/DWD/VAL/HOAPS Issue: 1.1 Date: 25.03.2011
---	---	---



A description of the parameters, their dependency on additional input data sources, the SSM/I raw data handling and FCDR production, their continuation with future HOAPS releases and the HOAPS versioning approach is given in the product user manual [RD 2]. Basic accuracy requirements are defined in the product requirements document [RD 1], and the algorithm theoretical basis document describes the individual parameter algorithms [RD 3].

1.1 Applicable documents

Reference	Title	Code
AD 1	Memorandum of Understanding between CM SAF and the Max-Planck Institute for Meteorology and Meteorological Institute, University of Hamburg	
AD 2	EUMETSAT CM SAF CDOP Product Requirements Document (PRD)	SAF/CM/DWD/PRD/1.7
AD 3	Cooperation Agreement	

1.2 Reference Documents

Reference	Title	Code
RD 1	CM-SAF Product Requirements Document	SAF/CM/DWD/PRD/1.6
RD 2	Product User Manual	SAF/CM/PUM/HOAPS/1.0
RD 3	Algorithm Theoretical Basis Document HOAPS	SAF/CM/ATBD/HOAPS/1.0

 	EUMETSAT SAF on CLIMATE MONITORING Validation Report HOAPS release 3.2	Doc.No.:SAF/CM/DWD/VAL/HOAPS Issue: 1.1 Date: 25.03.2011
---	---	--

2 The EUMETSAT SAF on Climate Monitoring

The importance of climate monitoring with satellites was recognized in 1999 by EUMETSAT Member States when they amended the EUMETSAT Convention to affirm that the EUMETSAT mandate is also to contribute to the operational monitoring of climate and the detection of global climatic changes". Following this, EUMETSAT established within its Satellite Application Facility (SAF) network a dedicated centre, the SAF on Climate Monitoring (CM SAF, <http://www.cmsaf.eu>). Since the start of the CM SAF in 1999 the project went through three phases, i.e., the Development Phase lasting from 1999 to 2004, the Initial Operations Phase (IOP) and the Continued Development and Operations Phase (CDOP). The consortium of CM SAF currently comprises the Deutscher Wetterdienst (DWD) as host institute, and the partners from the Royal Meteorological Institute of Belgium (RMIB), the Finnish Meteorological Institute (FMI), the Royal Meteorological Institute of the Netherlands (KNMI), the Swedish Meteorological and Hydrological Institute (SMHI) and the Meteorological Service of Switzerland (MeteoSwiss).


After focusing on the development of retrieval schemes to derive a subset of Essential Climate Variables (ECVs) in the development phase, CM SAF delivered to its users products based on Meteosat and polar orbiter data for Europe and Northern Africa supporting NMHSs in their provision of climate services in the IOP from 2004 to 2007. During CDOP, lasting from 2007 to 2012, the product validation continued, the time series were expanded and algorithms were further improved, while the study domain was extended from the baseline area to the MSG disk for the geostationary products and to include global and Arctic coverage for the polar orbiter products. In addition, long term climate datasets from polar orbiting and geostationary satellites are being generated for climate monitoring (i.e. HOAPS, METEOSAT and AVHRR-GAC based products).

A catalogue of available CM SAF products is available via the CM SAF webpage, <http://www.cmsaf.eu/>. Here, detailed information about product ordering, add-on tools, sample programs and documentation are provided.

3 Introduction

The Special Sensor Microwave Imager (SSM/I) radiometer aboard the Defense Meteorological Satellite Program (DMSP) satellites, available since 1987, became a foundation for the derivation of surface flux and precipitation time series by various international research groups. Depending on the dataset application purpose, blending and morphing techniques have been developed to combine different satellite and model data with the SSM/I time series.

Generally these datasets fall into two categories providing either surface fluxes or precipitation estimates. Prominent surface flux products are the Goddard Satellite-Based Surface Turbulent Fluxes version 2 (GSSTF2; Chou et al. 2003), the Japanese Ocean Flux Datasets with the Use of Remote Sensing Observations (J-OFURO 2; Kubota and Tomita 2007), the objectively analyzed air-sea fluxes (OAFlux; Yu and Weller 2007; Yu et al. 2008), and the merged flux dataset of the Institut Français de Recherche pour l'Exploration de la Mer (IFREMER; Bentamy et al. 2003). Well-known and widely used precipitation products for a variety of applications are the Global Precipitation Climatology Project (GPCP; Huffman et al. 1997; Adler et al. 2003), the Tropical Rainfall Measuring Mission (TRMM) Multisatellite Precipitation Analysis (TMPA; Huffman et al. 2007), the Climate Prediction Center (CPC) Merged Analysis of Precipitation (CMAP; Xie and Arkin 1997), the Unified Microwave

	EUMETSAT SAF on CLIMATE MONITORING Validation Report HOAPS release 3.2	Doc.No.:SAF/CM/DWD/VAL/HOAPS Issue: 1.1 Date: 25.03.2011
---	---	--

Ocean Retrieval Algorithm (UMORA; Hilburn and Wentz 2008), the Global Satellite Mapping of Precipitation (GSMaP; Kubota et al. 2007), and Precipitation Estimation from Remotely Sensed Information using Artificial Neural Networks (PERSIANN; Hsu et al. 1997).

The combination of such satellite-retrieved datasets results in estimates of the global ocean freshwater flux. Schlosser and Houser (2007) state that this is a highly required but difficult task, as differently calibrated time series and inhomogeneous data sources have to be combined while there is no comprehensive in situ validation data available.

Alternatively, reanalysis datasets, such as the 40-yr European Centre for Medium-Range Weather Forecasts (ECMWF) Re-Analysis (ERA-40) (Uppala et al. 2005) and ERA-Interim (ERA-Interim; Simmons et al. 2007), National Centers for Environmental Prediction (NCEP) NCEP-1 (Kalnay et al. 1996), NCEP-2 (Kanamitsu et al. 2002), or the Japanese 25-year Reanalysis (JRA-25) (Onogi et al. 2007), provide the relevant water cycle parameters.



For the ocean surface fluxes, ship observations give the opportunity to derive global ocean datasets, such as the National Oceanography Centre Southampton (NOCS) surface flux dataset (Berry and Kent, 2009).

In contrast, the Hamburg Ocean Atmosphere Parameters and Fluxes from Satellite Data (HOAPS) has been developed with the goal to derive the parameters required to retrieve the global ocean surface freshwater flux components consistently within one entirely satellite based dataset (Andersson et al., 2010b). For the sake of long-term homogeneity the approach for HOAPS is to use the SSM/I as the common data source for all retrievals instead of combining different data sources. This ensures a uniform sampling for all parameters and avoids complications with the cross calibration and the implementation of retrieval procedures for different types of sensors. Another criterion for the design of the dataset is to use stand-alone retrieval procedures that only rely on SSM/I brightness temperatures and the Advanced Very High Resolution Radiometer (AVHRR)-based SST as input and are independent of ancillary input data, such as additional first guess fields from model output.

Previous studies (e.g., Brunke et al. 2002; Chou et al. 2003, 2004) indicate large deviations in the comparison of different flux datasets. From a comparison with buoy data Bourras (2006) assumed the overall regional accuracy of satellite-derived fluxes to be in the order of 20%–30%. To use satellite-derived fluxes for quantitative analyses, Bourras (2006) suggests that these errors need to be 5%–10% lower.

Similar numbers were found in comparisons for satellite-derived precipitation datasets (e.g., Adler et al. 2001; Beranger et al. 2006). In particular, the tropical regions and the high latitudes are prone to large differences between precipitation estimates. Moreover, reanalysis based estimates of evaporation and in particular precipitation tend to perform poor over the oceans because of the limited availability of assimilated in situ data over the oceans. The lack of long-term ground truth data with good spatial coverage is also the reason why validation studies over the ocean are difficult. The coverage of ship data often strongly depends on the general shipping routes, leading to larger errors in regions with sparse sampling. To date, inter-comparison studies are the most appropriate way of global-scale evaluation for evaporation and precipitation products to assess their systematic differences as a measure of methodological uncertainties.

Several recent readily available products are selected for comparison. These products are derived from different data sources and represent model-based estimates from a reanalysis dataset, in situ measurements from ships, and different satellite-based datasets that include

 	EUMETSAT SAF on CLIMATE MONITORING Validation Report HOAPS release 3.2	Doc.No.:SAF/CM/DWD/VAL/HOAPS Issue: 1.1 Date: 25.03.2011
---	---	--

sensors not utilized in HOAPS. For the evaporation these are the ERA-Interim reanalysis, the ship-measurement based NOCS V2 dataset, and the satellite-data based IFREMER V3 flux dataset. The HOAPS precipitation product is compared to ERA-Interim and the two satellite-based products, GPCP V2 and TRMM 3B43.

Also, the input parameters for the evaporation retrieval, wind, and near surface specific humidity are assessed. All used time series have a temporal overlap with HOAPS of more than one decade from January 1992 to December 2005. The resulting comparison period of 14 years is an advance over previous studies that are mostly limited to substantially shorter time periods. However, some of these estimates are not fully independent as input data from the same observations might have been used. Scatterometer wind speeds or ship observations are, for example, assimilated into the ERA-Interim reanalysis and SSM/I brightness temperatures are used in ERA-Interim and also in the satellite-based products.

An overview of the datasets used in this study is given in section 4. The climatological comparisons between HOAPS and the other products are shown in section 5 together with a discussion of the results and implications for the individual parameters. Section 6 presents the results on the decadal stability. Finally, a conclusion and outlook is given in section 7.

4 Data Sets for Comparison with HOAPS

4.1 IFREMER Satellite Derived Turbulent Fluxes V3



Bentamy (2003) developed a remotely sensed data set of wind stress and surface turbulent latent and sensible heat fluxes. Here the version 3.0 is used, which is currently available for the time period from March 1992 to December 2007 (Bentamy, 2008). It utilizes different input sources to derive the flux parameters using the COARE 3.0 algorithm (Fairall, 2003). As in HOAPS, q_{air} is derived from SSM/I data with the algorithm described in Bentamy (2003). In contrast to HOAPS, the IFREMER wind speed is derived from a combination of retrievals based on scatterometers and SSM/I data. The flux fields are retrieved using a kriging method to merge the various satellite estimates. The SST is taken from the NOAA - Optimum Interpolation (OI) weekly product.

4.2 NOCS v2.0

The National Oceanography Centre Southampton (NOCS) v2.0 surface flux dataset by Berry and Kent (2009) is exclusively based on Voluntary Observing Ship (VOS) data from the International Comprehensive Ocean–Atmosphere Data Set (ICOADS; Worley et al. 2005). The NOCS dataset provides fields of marine surface meteorology and fluxes over the global ocean that are constructed using a bias adjustment procedure and an optimum interpolation method. The turbulent fluxes are derived with the bulk parameterization of Smith (1980,1988).

4.3 GPCP V2

The GPCP version 2 combined product (Adler et al. 2003) provides fields of satellite-derived precipitation retrieved from passive microwave and infrared data. For the merging procedure the infrared precipitation estimates from geosynchronous satellites are constantly calibrated with the passive microwave precipitation retrievals from polar orbiting satellites, which are considered to be of higher accuracy. Different from HOAPS, GPCP provides also precipitation observations over land, where the analysis also makes use of surface data from rain gauges.

 	EUMETSAT SAF on CLIMATE MONITORING Validation Report HOAPS release 3.2	Doc.No.:SAF/CM/DWD/VAL/HOAPS Issue: 1.1 Date: 25.03.2011
---	---	--

4.4 TRMM 3B43

In the 3B43 product, data from the TRMM Microwave Imager (TMI) and the Precipitation Radar (PR) are blended with SSM/I and geosynchronous precipitation data. In analogy to the GPCP product, microwave and infrared retrievals are used to complement the TRMM precipitation retrievals. The TRMM Combined Instrument (TCI) precipitation data from PR and TMI are used as the calibration reference for the microwave and infrared retrievals to derive a “best-estimate precipitation rate.” The 3B43 product is available for the period after 1998 and is limited to the region between 50°S and 50°N.

4.5 ERA-Interim

ERA-Interim is the latest and improved global atmospheric reanalysis dataset provided by the ECMWF (Simmons et al. 2007). It uses an advanced data assimilation scheme and additional observations from various sources compared to ERA-40. At present the ERA-Interim record starts at 1989. Fields of wind speed, q_{air} , evaporation, and precipitation were obtained from the 12-h forecast. As a q_{air} parameter for the near-surface layer is not directly available in the ERA-Interim archive, it was calculated from the 12-h forecast values of 2-m air temperature, 2-m dewpoint temperature, and surface pressure.

5 Evaluation of HOAPS Parameters

5.1 Methodology

For the following comparisons a common time period from 1992–2005 is chosen, which is covered by all datasets except for the TRMM product, which starts only in 1998. Since TRMM products are the only long-term satellite-based precipitation dataset that includes precipitation radar data, it is included in the comparisons.

The HOAPS land–sea and ice masks were applied to all datasets to achieve a common spatial coverage of the global ice-free oceans. Apart from the differences of the mean fields for the 1992–2005 period, the respective zonal means have been calculated as well as the time series of the monthly global mean values.

For ERA-Interim the ocean surface freshwater flux fields were calculated by subtracting the respective evaporation and precipitation monthly mean grid values. Additionally, the IFREMER evaporation and GPCP precipitation were subtracted from each other to provide a second freshwater flux product for comparison.

5.2 Near surface specific humidity

HOAPS climatological mean near-surface atmospheric specific humidity (q_{air}) and its yearly cycle is shown in Figure 1. The highest values of up to 20 g/kg of the climate mean q_{air} are found in the tropical warm pool region and the ITCZ. Toward the subtropical regions the values steeply decrease below 2 g/kg. The annual cycle (Figure 1, right panel) clearly shows the movement of the tropical q_{air} maximum with the position of the sun.

The comparison of q_{air} between HOAPS and ERA-Interim (Figure 2, top left) exhibits the most distinct differences in the tropical and subtropical regions. Positive biases in the warm pool region exceed 1 g/kg (<10%) and reach 2 g/kg (20%) over the eastern Atlantic and eastern Pacific. In the subtropical central Pacific between 10° and 20° HOAPS q_{air} is systematically lower compared to ERA-Interim on both hemispheres.

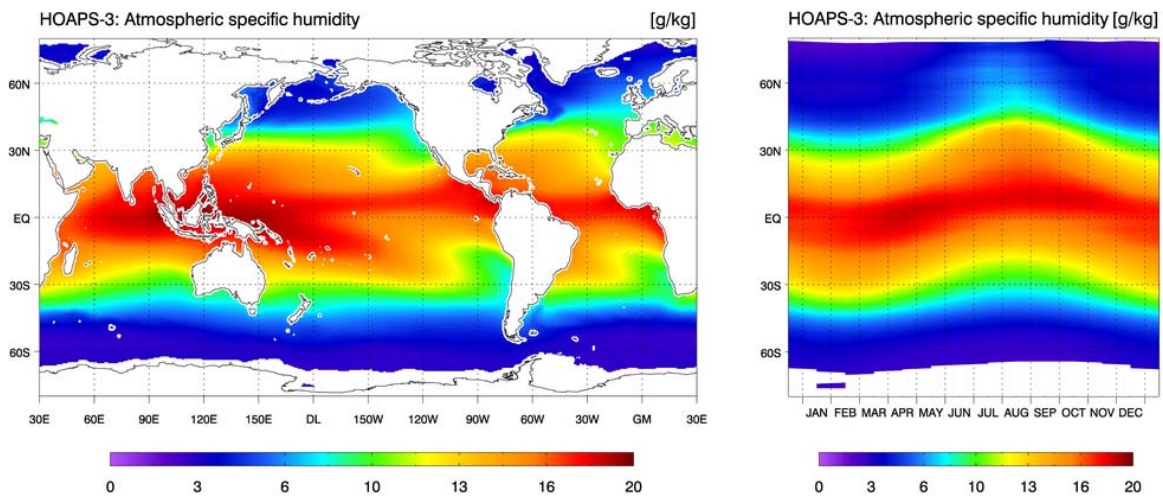


Figure 1: Climatological mean field (left) and zonal mean annual cycle (right) of HOAPS near surface specific humidity q_{air} for the years 1988–2005.

The comparison with NOCS (Figure 2, top right) reveals a similar pattern that is shifted toward a more negative bias. In particular in the subtropical regions HOAPS is partly more than 2 g/kg (20%) lower compared to NOCS. Between 40°S and 60°S NOCS is systematically higher compared to all other datasets by up to 1.5 g/kg (30%, locally up to 50%).

The HOAPS and IFREMER datasets use the same algorithm to derive q_{air} from SSM/I measurements (Bentamy et al., 2003). As may be expected, the comparison reveals only minor differences between both products. The deviations between HOAPS and IFREMER (Figure 2, lower right) are overall small with ± 0.5 g/kg in parts of the tropical regions and over the Kuroshio and Gulf Stream. This is within 5% for the most regions, locally within 10%. In the tropical belt the general tendency of the regional differences is similar to the previous comparisons, with IFREMER being much closer to HOAPS than to the other products.

The global mean time series of all datasets (Figure 2, lower left, top) agree in magnitude and variability with the NOCS dataset being slightly higher compared to the other datasets. Also the zonal mean values of all datasets (Figure 2, lower left, bottom) show very similar characteristics. The NOCS dataset is generally moister between 20° north and south compared to the satellite retrieval of Bentamy et al. (2003), which is used in HOAPS and IFREMER. Hence, the NOCS monthly global mean q_{air} values are on average 0.35 g/kg (3%) higher compared to HOAPS. ERA-Interim exhibits the lowest zonal mean values in the equatorial region as well as around 30° north and south, which results in global mean values that are on average 0.13 g/kg lower compared to HOAPS.

5.2.1 Discussion

The comparison of q_{air} from IFREMER and HOAPS exhibits only minor differences because of application of the same algorithm for SSM/I data. Hence, the deviations originate either from different sensor calibrations in the individual SSM/I brightness temperature records or from a different sampling due to the kriging technique used in the IFREMER dataset.

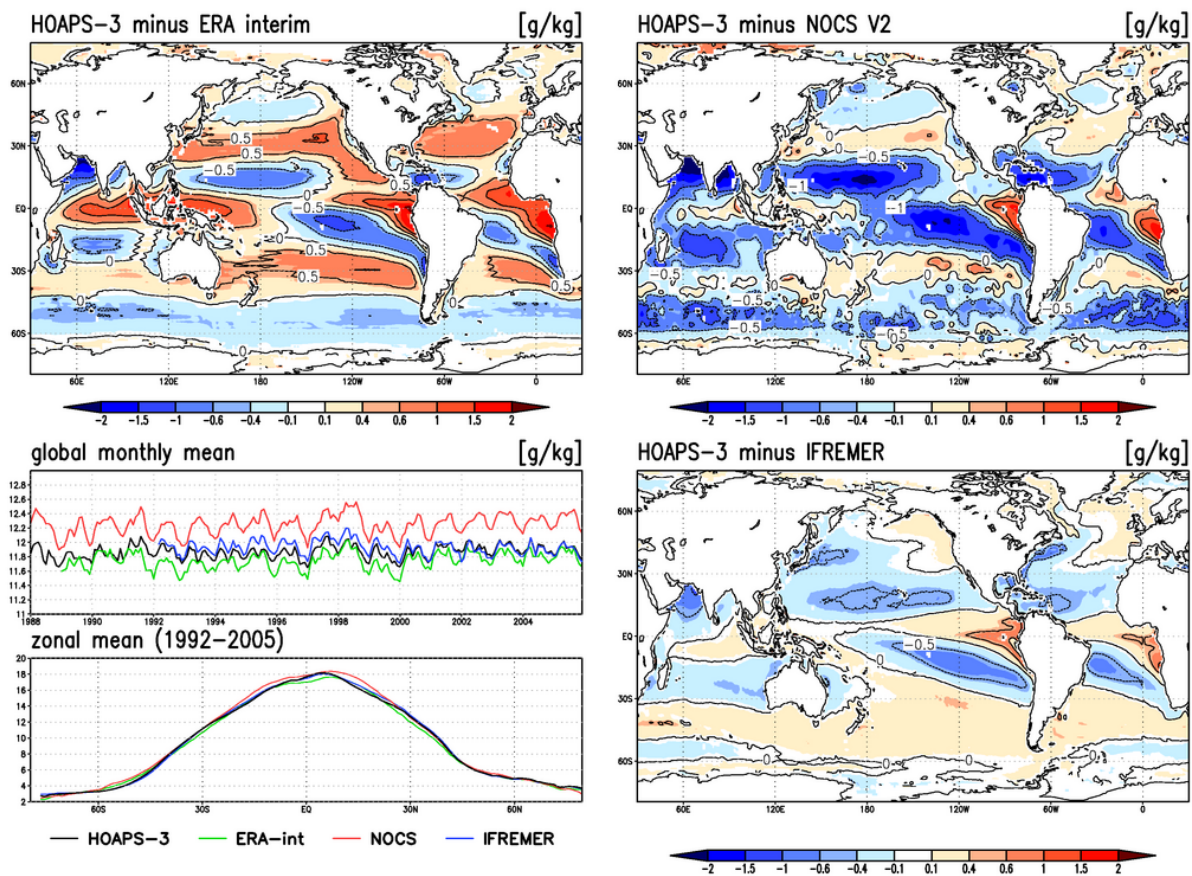


Figure 2: Difference of the 1992-2005 climate mean HOAPS near surface specific humidity and ERA interim (upper left), NOCS v2.0 (upper right), and IFREMER Flux (lower right). The lower left panel shows the global monthly mean humidity time series of each data set and the zonal mean humidity for the overlapping time period 1992-2005.

Larger deviations are found in the comparison with NOCS and ERA-Interim. In particular, over the subtropical regions, a strong negative bias in the IFREMER and HOAPS satellite retrieval compared to NOCS is evident, which is most expressed during the winter season of each hemisphere. Jackson et al. (2009) found similar patterns in the comparison of different q_{air} satellite retrievals with ICOADS ship and buoy data and related this dry bias to an underestimation of q_{air} by the Bentamy et al. (2003) algorithm in the range of 15–20 g/kg. In comparison of HOAPS with ERA-Interim this bias is less pronounced, since ERA-Interim is generally dryer in the tropical regions compared to NOCS.

Over the southern oceans, the poor sampling of the ship observations lead to larger

Table 1: Requirements for near surface humidity product CM-141 as given in the PRD [RD 1] Accuracy numbers are given for global mean values. Regional larger deviations may occur.

	Threshold	Target	Optimal
Bias	15%	4%	2%
RMS	20%	8%	5%
Decadal stability	1%	0.5%	0.26%

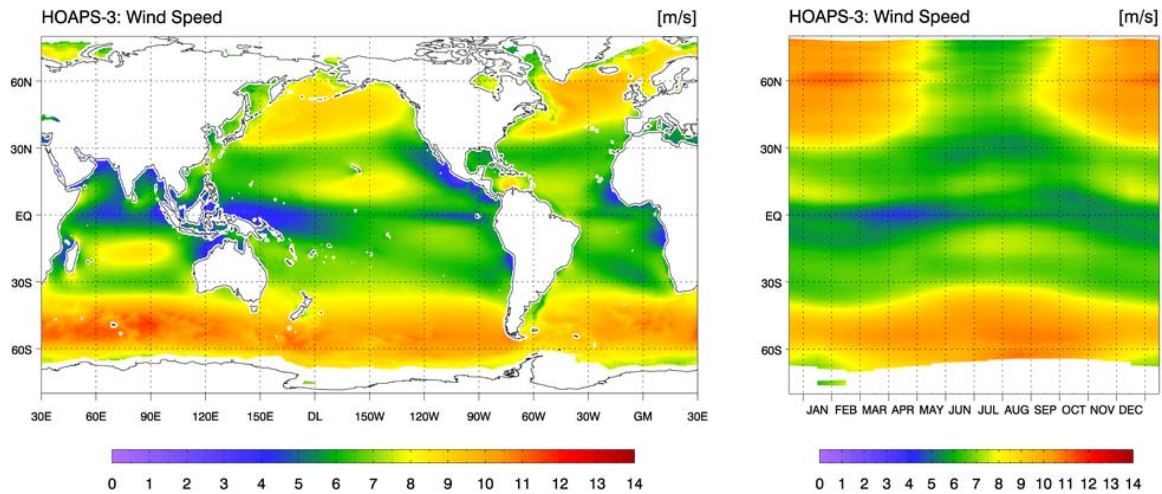


Figure 3: Climatological mean field (left) and zonal mean annual cycle (right) of HOAPS near surface wind speed for the years 1988–2005.

uncertainties in the NOCS dataset. Especially during cold seasons, ground observations are sparse, leading to large deviations between the datasets. Over the North Atlantic and Pacific, where the sampling is much better, this problem is not evident. However, the accuracy of satellite retrievals also depends on the representativeness of spatiotemporal variability of their a priori data used during the development of the algorithm. Moreover, the retrieval of q_{air} is not possible for weather situations with strong precipitation.

Based on the validation against the monthly mean in situ based NOCS dataset it can be concluded that the HOAPS near surface specific humidity fulfils the target requirement with a mean bias of -0.4 g/kg (3%) and an RMS value of 0.1 g/kg (1%) (Table 1, PRD [RD 1]).

5.3 Near surface wind speed

HOAPS climatological mean wind speed for the years 1988–2005 is shown in the left panel of Figure 3. North Atlantic and Pacific storm-track regions as well as the “roaring forties” and “furious fifties” over the Southern Ocean are characterized by maximum climate mean values of up to 14 m/s . Secondary local maxima exist in the tropical trade wind area. Moreover, the characteristic minima of the subtropical calms and the Southeast Asian warm pool region are clearly evident. The zonal mean annual cycle (Figure 3, right) highlights the wintertime maxima of wind speed in the mid- and high latitudes of both hemispheres, while only weak variability occurs in the subtropical regions.

The comparison of HOAPS wind speed with ERA-Interim, NOCS, and IFREMER is depicted in Figure 4. The top left panel shows the wind speed difference between HOAPS and ERA-Interim. Red colors indicate regions where HOAPS exhibits on average higher values, while in blue shaded regions HOAPS is lower than the compared dataset.

ERA-Interim wind speeds are generally lower compared to all other products over the global oceans. A mean bias of 0.60 m/s relative to HOAPS is found for the global ocean. A similar behaviour in the comparison of satellite retrieved wind speed with reanalysis data was found in earlier studies (Meissner et al. 2001; Kelly et al. 2001; Monahan 2006). Apart from the general bias, other distinct local differences in the comparison of HOAPS and ERA-Interim occur in the intertropical convergence zone (ITCZ), where ERA-Interim is significantly lower compared to the other datasets. In regions with cold surface currents, such as the Antarctic

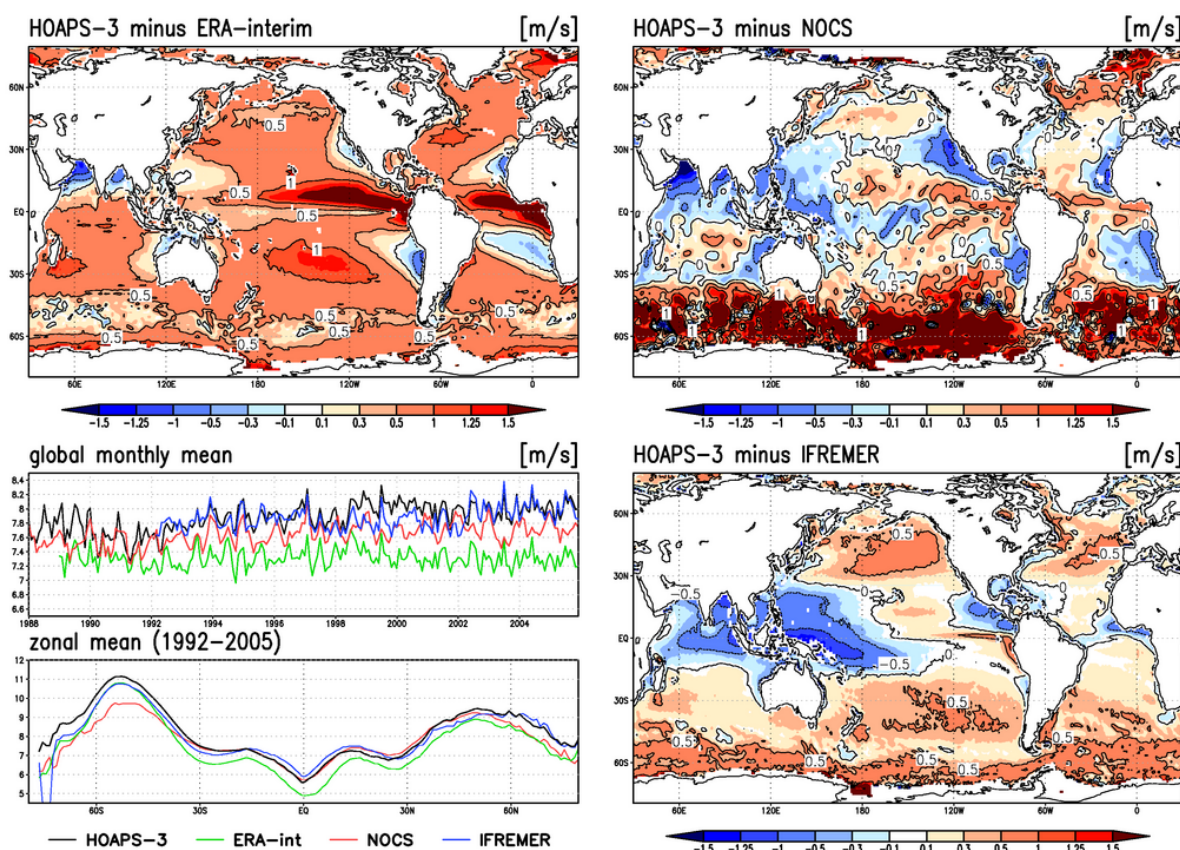


Figure 4: Difference of the 1992–2005 climate mean HOAPS wind speed and ERA-Interim (upper left), NOCS v2.0 (upper right), and IFREMER flux (lower right). The global monthly mean wind speed time series of each dataset (lower-left, top), and the zonal mean wind speed (lower-left, bottom) for the overlapping time period 1992–2005.

Circumpolar Current (ACC) or the upwelling regions on the western continental boundaries, HOAPS and ERA-Interim show comparable values within 0.5 m/s (5%). The largest negative bias is found over the Arabian Sea and over the Bay of Bengal.

Similar patterns but with smaller magnitude are evident in the difference plot of HOAPS and NOCS (Figure 4, top right). HOAPS wind speeds are about 1 m/s (10%) lower compared to NOCS at the western boundaries of the continents. Most notably, the IFREMER product exhibits a significant bias in the region of the precipitation maximum of the western tropical Pacific and the warm pool. The IFREMER wind speeds exceed HOAPS by up to 1.5 m/s (>20%) in this region.

Apart from the distinct differences over the warm pool and over the upwelling regions, the deviations between HOAPS, NOCS, and IFREMER are mostly below 0.5 m/s (<5%) in the tropics and mid-latitudes with the tendency of HOAPS to show slightly higher mean wind speeds. At high latitudes the NOCS dataset exhibits a systematic low bias compared to HOAPS and the other datasets. In particular over the Southern Ocean the NOCS wind speed appears to be systematically underestimated. This is also reflected in the total error estimate given in the NOCS dataset, which is around 3.5–4 m/s for the region south of 40°S, because of the sparse data sampling.

5.3.1 Discussion

The underestimation of ERA-Interim compared to all other datasets is known from previous studies comparing satellite-retrieved and reanalysis wind speeds (Meissner et al. 2001; Kelly et al. 2001; Monahan 2006). The systematic deviations are caused by the different principles used to determine the wind speed. Satellite observations measure the surface wind stress, which is then often recalculated to represent 10-m equivalent neutral-stability wind speed. In contrast to that, reanalysis models assimilate SSM/I radiances and scatterometer wind speed observations and can directly analyse and forecast the actual winds at 10 m. Another general source for systematic differences is that the reanalyses implement a static sea surface, while satellite measurements are sensitive to ocean surface currents and measure the wind speed relative to the underlying sea surface. Additionally, regionally limited measurements acquired by rawinsondes and the radiative transfer calculations underlying the satellite retrieval algorithms as well as the reanalyses lead to locally different results in the wind speed. The large differences over the monsoon regions of the Bay of Bengal and the Arabian Sea are likely to originate from lack of input data representing the specific atmospheric and sea surface properties in these regions due to atmospheric advection and oceanic upwelling.

The satellite-derived wind speed products, HOAPS and IFREMER, exhibit an overall better agreement with biases below 0.5 m/s for most regions. Over the Southeast Asian warm pool the IFREMER wind speed shows a high bias compared to the other datasets. In this region the sensitivity of the evaporation to the retrieved wind speed is high because of the generally low wind speeds in this region. Therefore, minor differences in wind speed could have a strong impact on the resulting evaporation estimates. The frequently strong precipitation in this region hampers the retrieval of wind speed using microwave radiometers, leading to gaps in the wind speed data. Filling these gaps with scatterometer-derived wind speeds as done in the IFREMER dataset may cause biases since the scatterometer wind speed algorithm can also be strongly affected by precipitation under certain circumstances. Under low wind speeds and when the scatter from the sea surface is low, additional volume scattering of even light precipitation leads to a spurious wind signal (e.g., Tournadre and Quilfen 2003; Wallcraft et al. 2009). An inverse effect is observed for high wind speed regimes. The NOCS dataset exhibits significant biases at high latitudes. The limited number of observations from these regions in the NOCS dataset is biased toward low wind speeds since ships tend to avoid storms and high sea state related to winds, particularly during the cold season. A similar, but considerably weaker, effect may occur in the HOAPS data because of strong precipitation, which inhibits the retrieval of wind speed from the satellite (Wentz 1997; Andersson et al. 2010b). However, this affects usually only the inner cores of precipitating weather systems and hence only a limited number of satellite observations. In regions with frequent precipitation, such as the ITCZ or the Southern Ocean, this is the case for 10%–15% of the

Table 2: Requirements for near surface wind speed product CM-142 as given in the PRD [RD 1]. Accuracy numbers are given for global mean values. Regional larger deviations may occur.

	Threshold	Target	Optimal
Bias	1 m/s	0.6 m/s	0.5 m/s
RMS	2.8 m/s	2.0 m/s	0.5 m/s
Decadal stability	0.2 m/s	0.1 m/s	0.04 m/s

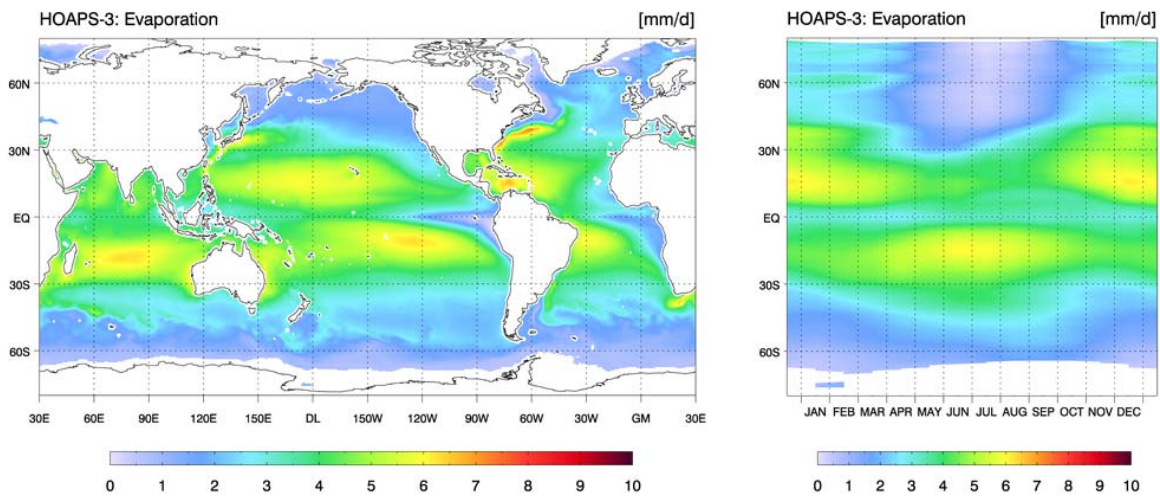


Figure 5: Climatological mean field (left) and zonal mean annual cycle (right) of HOAPS evaporation for the years 1988–2005.

observations.

Estimates of the accuracy of the HOAPS wind speed were carried out by Winterfeldt et al. (2010) who compared HOAPS, Quick Scatterometer (QuikSCAT)–SeaWinds scatterometer, and NCEP reanalysis wind speeds with buoy data over the North Sea and North Atlantic. The HOAPS wind minus observations showed RMS values of 2 m/s, which is comparable to the requirement for the scatterometer of the QuikSCAT mission and is regarded to be consistent with values from other studies. It is shown that the HOAPS wind retrieval performs equally well in near-coastal and remote ocean regions.

Based on the comparison of HOAPS monthly mean wind speed against the in situ based NOCS climatology, which shows an average bias of 0.24 m/s and an RMS value of 0.15 m/s, it can be concluded that the target requirements defined in the product requirement document are met. (Table 2, PRD [RD 1]).

5.4 Evaporation and Latent heat flux

The mean global ocean evaporation (Figure 5, left panel) shows the well-known climatological distributions with strong maxima over both hemispheres with values of up to 7 mm/day. Mid- and high latitudes exhibit generally lower values of less than 3 mm/day with the exception of the warm boundary currents of the Kuroshio, the Gulf Stream, and the Agulhas Current. The Gulf Stream generates the highest mean evaporation values on the globe of up to 8 mm/day. A pronounced seasonal variability can be identified in the climatological zonal mean annual cycle (Figure 5, right panel) with maximum evaporation values in the trade wind belts and secondary maxima in the mid- and high-latitude storm-track regions during the winter season of each hemisphere.

The difference patterns for all datasets in Figure 6, especially over the subtropics, are similar to the climatological mean field pattern of HOAPS evaporation (Figure 5). They show higher difference values in regions of large evaporation and smaller values in regions with low evaporation. Furthermore, the differences appear to be determined to a large extent by the humidity fields. This is most distinct in the comparison of HOAPS with NOCS and ERA-Interim, while the comparison with the IFREMER dataset exhibits some similar tendencies, but mostly smaller values below 1 mm/day. The magnitudes of the deviations are regionally

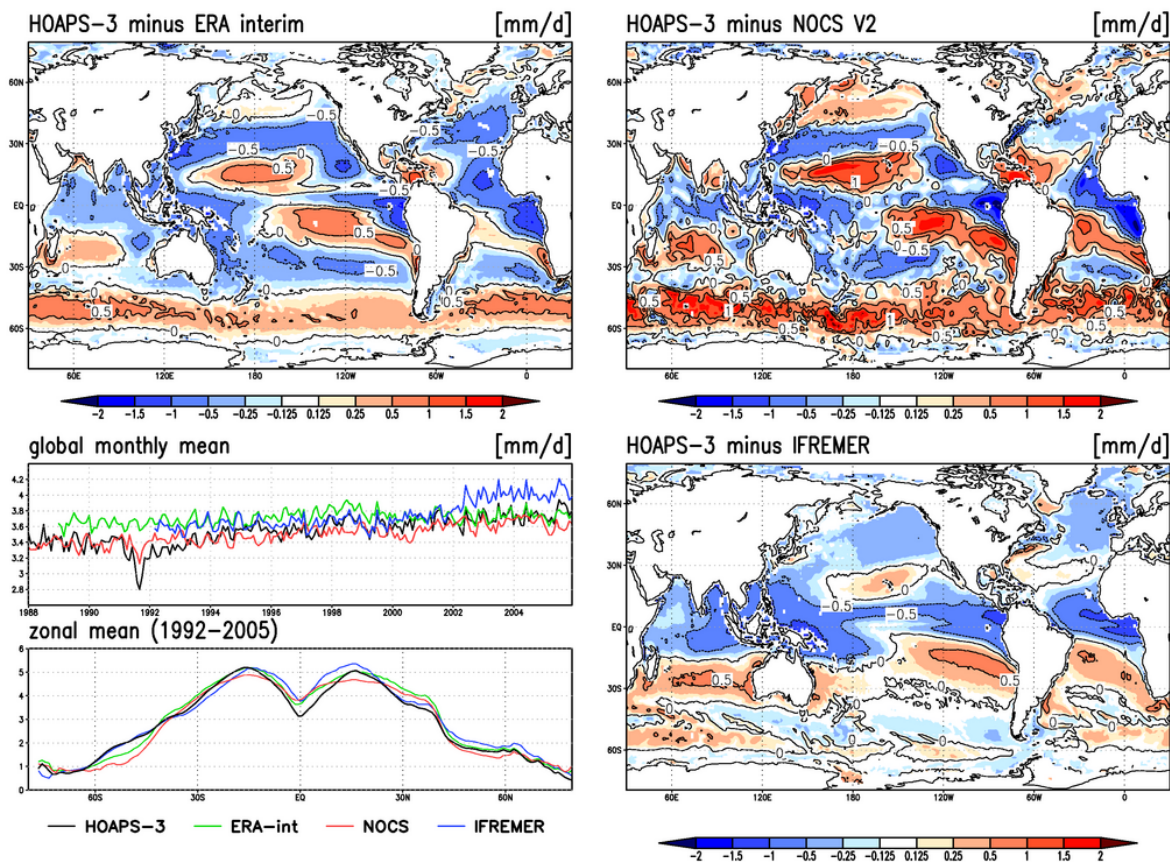




Figure 6: Difference of the 1992–2005 climate mean HOAPS evaporation and ERA-Interim (upper left), NOCS v2.0 (upper right), and IFREMER flux (lower right). The global monthly mean evaporation time series of each dataset (lower-left, top), and the zonal mean evaporation (lower-left, bottom) for the overlapping time period 1992–2005.

largest in the comparison with NOCS, reaching more than 1.5 mm/day or 20% of the average value. In the comparison with IFREMER the relative differences are generally below 5%–10%.

In a broad band from the Kuroshio over the North Pacific to the North American east coast ERA-Interim and NOCS evaporation is systematically higher compared to HOAPS. This pattern continues southward along the Baja California. Over the cold tongue in the eastern equatorial Pacific and the Southeast Asian warm pool HOAPS evaporation is systematically lower compared to all other datasets. Because of the fairly small absolute values of evaporation, the relative error reaches more than 30% in these regions.

An underestimation of HOAPS is evident in the eastern tropical Atlantic with differences of more than 1 mm/day (up to 50%) because of a combination of an overestimation of q_{air} along the West African coast and an underestimation of q_{sea} in the tropical and subtropical Atlantic. The latter effect can be identified in the difference of HOAPS and IFREMER evaporation fields, which is not influenced by strong q_{air} biases between these datasets as the same algorithm has been used (see section 5.2).

Over the North Atlantic and North Pacific between 40° and 80°N the comparison between the datasets shows mixed results with differences that are mostly below 0.5 mm/day. While the

 	EUMETSAT SAF on CLIMATE MONITORING Validation Report HOAPS release 3.2	Doc.No.:SAF/CM/DWD/VAL/HOAPS Issue: 1.1 Date: 25.03.2011
---	---	--

agreement of HOAPS is best with ERA-Interim, NOCS exhibits mostly lower values, and IFREMER tends to be slightly higher than HOAPS.

Over the storm tracks of the southern mid–high latitudes, NOCS and HOAPS exhibit the largest differences coinciding with the Southern Hemisphere’s band of strong winds between 40° and 60°S (see Figure 3). The mean evaporation of NOCS is locally more than 1.5 mm/day below HOAPS values, which corresponds to a relative difference of more than 50% in these regions. The corresponding error estimate given in the NOCS product exceeds 100%.

Compared to ERA-Interim, the HOAPS evaporation is up to 0.75 mm/day (more than 30%) higher for the southern midlatitude storm tracks. This is mainly related to differences in $q_{\text{sea}} - q_{\text{air}}$ (not shown), since HOAPS and ERA-Interim wind speed (Figure 4, upper left) agree well for this region.

The comparison of the climatological zonal means (Figure 6, lower left) shows an overall agreement in the location and magnitude of the maxima and minima of all datasets. In the southern midlatitudes HOAPS and IFREMER agree best, while ERA-Interim and NOCS exhibit significantly lower values. The largest deviations of up to 50% occur for the NOCS dataset in the data-sparse southern oceans and subtropics. In the tropical regions, the maxima in the NOCS dataset are less pronounced compared to the other datasets, while HOAPS exhibits the lowest values of all datasets around the equator. This is mainly due to the low bias over the tropical Atlantic and the cold tongue in the eastern tropical Pacific.

The magnitude of the global monthly mean time series is in close agreement for all datasets. In particular from 1995 onward, the biases are remarkably small. HOAPS and NOCS values are very close for the entire time series, except for the period after the eruption of Mount Pinatubo, when the HOAPS is impaired by a cold bias in the SST dataset (Andersson et al. 2010b). The major effect on the flux retrievals is evident before the start of the comparison time period in 1992. The sudden increase of the IFREMER time series in 2002 is likely to be an artefact from the wind or SST input data sources. However, this does not affect the general difference patterns.

The variability of the global monthly mean time series of HOAPS and IFREMER is very similar with a standard deviation of 0.18 mm/day. The corresponding values for NOCS and ERA-Interim are 0.13 and 0.09 mm/day, respectively. However, for the time period between 1995 and 2001 the standard deviations of all datasets range from 0.08 to 0.10 mm/day.

5.4.1 Discussion

In the comparison with three other datasets HOAPS shows a slight overall positive bias in regions with high values of evaporation and a somewhat lower negative bias in regions with low evaporation. When compared to the difference plots of wind speed and q_{air} , it appears that the large-scale deviations in evaporation in the tropical regions are primarily caused by differences of the q_{air} retrievals. The differences in the wind speed and q_{sea} are mostly of second-order importance, except for time period affected by the Mount Pinatubo eruption and the strong positive bias of the IFREMER dataset over the tropical warm pool. At higher latitudes, where the sea–air humidity difference is smaller, the influence of the wind speed increases.

The regional deviations in the comparison of HOAPS with ERA-Interim and NOCS are larger as compared to the IFREMER product, which turns out to be most consistent with HOAPS. The global mean evaporation for all compared products differs less than 10% for most of the investigated time period from 1992 to 2005. This is in accordance with results for global

mean estimates of Trenberth et al. (2009) who found similar differences between satellite- and model-based datasets.

Several comparison studies for global ocean evaporation and latent heat flux datasets have been carried out, such as Bourras (2006) and Liu and Curry (2006). These include HOAPS version 2 fluxes, which do not substantially differ from HOAPS values as the flux parameterization scheme did not change since this version and the used Pathfinder SST dataset versions are comparable. In these comparisons HOAPS fluxes already showed good performance. Especially, Bourras (2006) compared five satellite-derived latent heat flux products (HOAPS-2, the Japanese Ocean Flux Datasets with Use of Remote Sensing Observations (J-OFURO; Kubota et al. 2002), the Jones dataset (Jones et al. 1999), the Goddard Satellite-Based Surface Turbulent Fluxes, version 2 (GSSTF-2; Chou et al. 2003), and the Bourras–Eymard–Liu dataset; Bourras et al. 2002) and concluded that HOAPS is the most appropriate product to study turbulent fluxes over the world oceans.

The reasons of uncertainties in the evaporation estimates point at the retrieval of the relevant parameters wind speed, q_{air} , and SST that are affected by precipitation and clouds. Depending on the methodology and sampling density this may lead to errors in the absolute values and the temporal variability in regions with persistent cloud cover and frequent precipitation. Wind speed and q_{air} cannot reliably be retrieved under strong precipitation. Similar to the SST, missing values may be interpolated as it is done in the IFREMER product by a kriging procedure. In HOAPS the missing values for q_{air} and wind speed are not interpolated resulting in a considerably lower number of evaporation observations in regions with frequent precipitation. The strongest effect is observed over the Southern Ocean, the ITCZ, and tropical warm pool, where in 10%–15% of all SSM/I observations the retrieval of wind speed q_{air} and hence evaporation is not possible.

The systematic omission of potentially extreme deviations from the mean values or from the surrounding area may result in unintended biases. A back of the envelope maximum error estimate indicates already that even under the extreme assumption (100% error of evaporation estimate) would not result in more than about 10% error for the monthly mean in the most affected regions.

Based on the comparison of HOAPS monthly mean evaporation (latent heat flux) against the in situ based NOCS climatology, it can be concluded that the target requirements defined in the product requirement document are met with a mean bias of 0.04 mm/d (1%) and a RMS value of 0.13 mm/d (3.7%). The corresponding values for latent heat flux are 1 W/m² and 3.7 W/m² respectively (Table 3, PRD [RD 1]).

Table 3: Requirements for evaporation (CM-143) and latent heat flux (CM-145) products as given in the PRD [RD 1]. Accuracy numbers are given for global mean values. Regional larger deviations may occur.

	Threshold	Target	Optimal
Bias	1 mm/d 22 W/m ²	0.25 mm/d 8 W/m ²	0.15 mm/d 5 W/m ²
RMS	1.4 mm/d 30 W/m ²	0.5 mm/d 15 W/m ²	0.3 mm/d 10 W/m ²
Decadal stability	0.1 mm/d 3 W/m ²	0.015 mm/d 0.8 W/m ²	0.002 mm/d 0.1 W/m ²

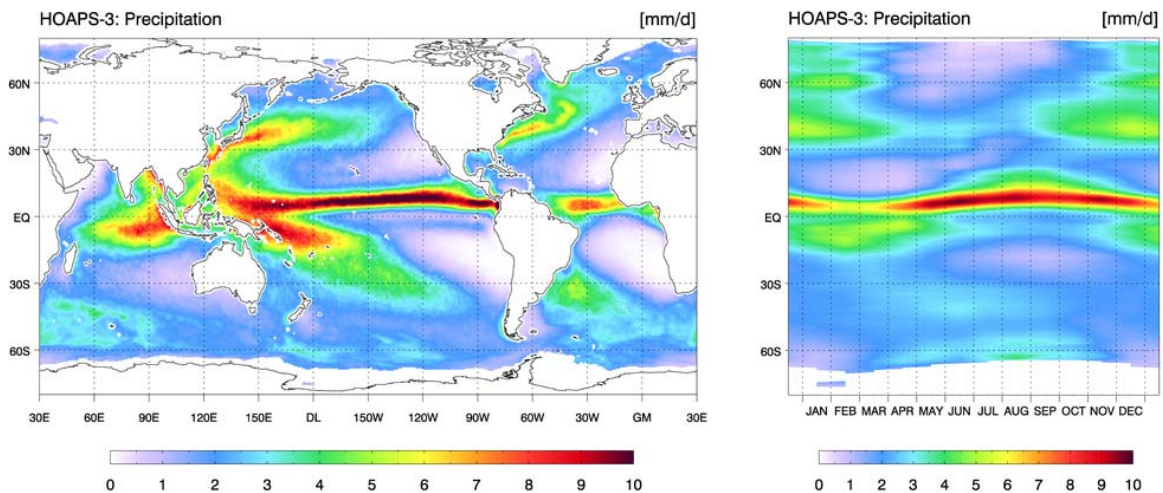


Figure 7: Climatological mean field (left) and zonal mean annual cycle (right) of HOAPS precipitation for the years 1988–2005

5.5 Precipitation

The climatological mean precipitation from HOAPS (Figure 7, left panel) well represents the known global distribution of precipitation. Dominant features are the overall highest rain rates in the ITCZ, exceeding 10 mm/day, and the regional maxima over the tropical Indian Ocean and the South Pacific convergence zone (SPCZ). The North Atlantic and Pacific storm tracks are also clearly identifiable with maximum values of up to 9 mm/day over the Gulf Stream and Kuroshio currents. Global precipitation minima can be observed in the so called subtropical oceanic deserts in the eastern subtropical Atlantic and Pacific.

The zonal mean annual cycle (Figure 7, right panel) clearly shows the seasonal displacement of the ITCZ as well as the high precipitation values over the Northern Hemisphere storm tracks during the cold season. Also the development of the Southern Hemisphere subtropical maximum in the SPCZ between January and April is evident.

ERA-Interim precipitation is generally higher on global scale compared to all satellite-derived products as depicted in the difference plot of HOAPS and ERA-Interim and the global monthly mean time series of the datasets in Figure 8. This bias originates mainly from the tropical belt, where ERA-Interim exceeds HOAPS partly by more than 2 mm/day (up to 50%). The issue of excessive tropical precipitation is already known from the former ERA-40 reanalysis. However, the tropical moisture budget in ERA-Interim appears to be improved over ERA-40, for which this positive bias was even stronger (Simmons et al. 2007). Except for the large tropical biases, the deviations between HOAPS and ERA-Interim are small and remain mostly below 1 mm/day (<20%). HOAPS precipitation values are noticeably larger compared to ERA-Interim over the Gulf Stream and Kuroshio currents as well as over the ITCZ region of the central Pacific and the southeastern tip of the SPCZ.

The difference map between HOAPS and TRMM 3B43 precipitation (Figure 8, upper right) shows in many regions a good agreement between both datasets with deviations below 0.5 mm/day (5%–10%) for most regions. Regionally larger differences are found in regions of high variability over the western Pacific, the SPCZ, and the Indian Ocean. In these regions HOAPS precipitation exceeds the TRMM product by up to 1 mm/day. However, because of the high mean values of precipitation the relative deviation remains below 20%. The largest

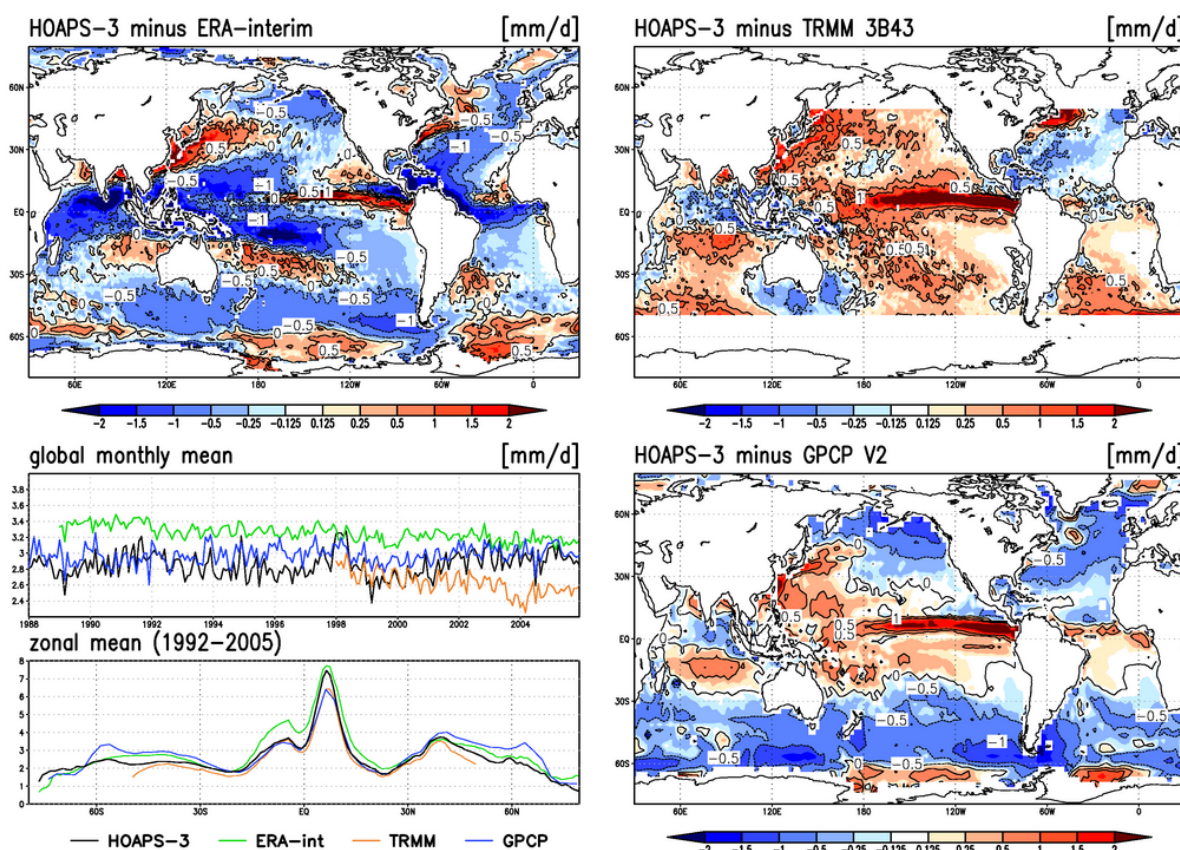


Figure 8: Difference of the 1992–2005 climate mean HOAPS precipitation and (upper left) ERA-Interim, (upper right) TRMM 3B43 (1998–2005), and (lower right) GPCP V2. The lower-left panel shows the global monthly mean precipitation time series of each dataset and the zonal mean precipitation for the overlapping time period 1992–2005 (1998–2005 for TRMM 3B43).

absolute difference is found in the central Pacific ITCZ where HOAPS exceeds TRMM by more than 2 mm/day (locally up to 50%). Over the entire North Atlantic basin, HOAPS precipitation is systematically lower compared to the TRMM data, except for the Gulf Stream region. Other regions with lower precipitation in HOAPS are found in the region south of Australia and the northern Indian Ocean.

The comparison of HOAPS with GPCP V2 (Figure 8, lower right) exhibits similar differences for the tropical belt as the comparison of HOAPS and TRMM. In the subtropical regions HOAPS precipitation is slightly larger than GPCP by values around 0.5 mm/day (10%). The maximum deviation of about 1.5 mm/day (30%–40%) is found in the Pacific ITCZ. Over the mid–high latitudes between 40° and 70° the precipitation in GPCP is systematically 10%–30% higher compared to HOAPS. Locally the values exceed 50%.

The global mean time series (Figure 8, lower left) of the satellite-derived products exhibit values around 3 mm/day, while the ERA-Interim record is constantly higher with 3.4 mm/day at the beginning of the time series and 3.2 mm/day at the end of the record. The month-to-month variability of the HOAPS record is slightly larger compared to the other datasets. The standard deviation of the monthly global mean values for HOAPS is 0.16 mm/day for the entire record compared to 0.11 and 0.12 mm/day for GPCP and ERA-Interim, respectively. The TRMM product, which is limited to 50° north and south and starts only in 1998, exhibits

a standard deviation of 0.15 mm/day. The corresponding value for HOAPS during this time period is 0.23 mm/day.

For the zonal means (Figure 8, lower left), the consistency among the satellite-derived products is best between 40° north and south. The overall bias in this region is low and the tropical and subtropical minima and maxima agree in location and magnitude for these datasets, apart from the northern branch of the ITCZ, which is stronger expressed in HOAPS. For the latter HOAPS agrees with ERA-Interim, which, however, exhibits generally higher values compared to the satellite products between 30° north and south. In the extratropical regions ERA-Interim tends to agree better with the satellite products, including HOAPS. However, the relative differences between the products increase toward higher latitudes.

5.5.1 Discussion

The comparison of HOAPS precipitation with the ERA-Interim reanalysis and the two satellite-retrieved climatological products, GPCP V2 and TRMM 3B43, exhibits considerable absolute differences in regions with high precipitation variability. The largest absolute differences are found over the ITCZ, while the relative differences are largest at high latitudes. This is in agreement with previous inter-comparison studies that included satellite-based as well as model-based precipitation estimates. These showed regionally large differences among the individual products that are up to 50% in regions of strong precipitation and at high latitudes (e.g., Adler et al. 2001; Klepp et al. 2005; Beranger et al. 2006). Particularly in the tropical regions model-based data (e.g., reanalysis products) are found to perform significantly poorer than satellite-derived fields (Trenberth and Guillemot 1998; Janowiak et al. 1998; Shinoda et al. 1999).



HOAPS precipitation turns out to be substantially higher compared to the other datasets in the Pacific ITCZ, while the precipitation in subtropical regions agrees well. At higher latitudes between 40° and 70° north and south, GPCP V2 exhibits a known high bias compared to HOAPS poleward, while being significantly lower in polar regions (Klepp et al. 2010). In the latitudinal bands from 40° to 70° GPCP utilizes Television and Infrared Observation Satellite (TIROS) Operational Vertical Sounder (TOVS) infrared data to compensate deficiencies in the GPCP high-latitude microwave-based retrievals (Adler et al. 2003). At midlatitudes the TOVS data are adjusted to the SSM/I estimates. Toward the poles the adjustment is transitioned to a bias adjustment based on rain gauges. At high latitudes from 70° and beyond the adjustment is done using land-based rain gauge data.

Comparisons with TRMM products should give deeper insight in the quality of HOAPS precipitation values because of the calibration of the TRMM product with the precipitation radar. In general, the HOAPS precipitation is slightly higher than the TRMM product. This may be in part attributed to a conspicuous decrease in the TRMM 3B43 time series since 2003. This decrease is likely to be caused by the introduction of the Advanced Microwave

Table 4: Requirements for precipitation product CM-144 as given in the PRD [RD 1].

Accuracy numbers are given for global mean values. Regional larger deviations may occur.

	Threshold	Target	Optimal
Bias	1.6 mm/d	0.25 mm/d	0.1 mm/d
RMS	2.25 mm/d	0.5 mm/d	0.2 mm/d
Decadal stability	0.03 mm/d	0.015 mm/d	0.002 mm/d

 	EUMETSAT SAF on CLIMATE MONITORING Validation Report HOAPS release 3.2	Doc.No.:SAF/CM/DWD/VAL/HOAPS Issue: 1.1 Date: 25.03.2011
---	---	--

Sounding Unit-B (AMSU-B) data to the TRMM dataset in 2001–2003, which gradually introduced a low bias of about 10% (GSFC 2007). The effect can also be identified in the global mean time series in the lower-left panel of Figure 8. When the time series is limited to 1998–2003, the deviations in the subtropical regions are reduced to values around 0.2 mm/day.

Because of the lack of reliable in situ measurements detailed quantitative comparisons for oceanic precipitation are rare and validation efforts are still mostly limited to short period regional inter-comparison studies. Moreover, the strong spatial and temporal variability of the precipitation complicates such validation efforts.

In particular the availability of reliable ground data for validation studies is very limited. The only frequent measurements in the central Pacific are taken by several rain gauges on buoys of the Tropical Atmosphere Ocean (TAO) project and precipitation radars on atolls. The representativeness of measurements from these systems is limited by their spatial restriction and the need of wind corrections for gauge under-catchment. But as these are the only available precipitation dataset, several studies evaluated satellite-based precipitation products using the atoll and buoy data. The results indicate a possible systematic underestimation of inner tropical precipitation up to 15% by various satellite retrievals (Adler et al. 2001, 2003; Bowman et al. 2009; Sapiano and Arkin 2009). In contrast to that, the new HOAPS retrieval exhibits mostly higher mean precipitation values in this region.

For the mid–high latitudes detailed case study analyses on midlatitude cyclones with intense postfrontal mesoscale convective mixed-phase precipitation were carried out by Klepp et al. (2003). Utilizing in situ voluntary observing ship data, it was shown that, in contrast to other satellite products, HOAPS recognizes small-scale intensive precipitation systems in cold air outbreaks with reliable patterns and intensities. This type of precipitation is also mostly missing in a large sample of events investigated in the ECMWF numerical weather prediction and ERA-40 reanalysis datasets (Klepp et al. 2005). Furthermore, Klepp et al. (2010) demonstrates the ability of HOAPS to detect even light amounts of cold season snowfall with a high accuracy of 96% between point-to-area collocations of ship-based optical disdrometers and satellite data.

Also for the North Atlantic region, Andersson et al. (2010a) carried out an analysis of the HOAPS precipitation variability connected to the North Atlantic Oscillation. It is shown that the response of precipitation structures to the atmospheric fluctuations is well represented in HOAPS and that the HOAPS precipitation fields showed convincing consistency with land-based rain gauge data in magnitude and variability.

Because of the lack of reliable in situ measurements the validation of HOAPS monthly mean precipitation is done against other satellite based climatologies and reanalysis data. The well established GPCP product is taken as the reference, because the TRMM product time series is relatively short and moreover it shows the discussed unrealistic decrease in 2003. Comparing HOAPS precipitation against the GPCP climatology shows a mean bias of -0.12 mm/d and a RMS value of 0.14 mm/d and it can be concluded that the target requirements defined in the product requirement document are met. (Table 4, PRD [RD 1]).

5.6 Freshwater Flux

The difference between evaporation and precipitation yields the oceanic freshwater flux into the atmosphere. Dominant features of either precipitation or evaporation fields determine the resulting global distribution of the freshwater flux as shown in Figure 9. A net flux into the

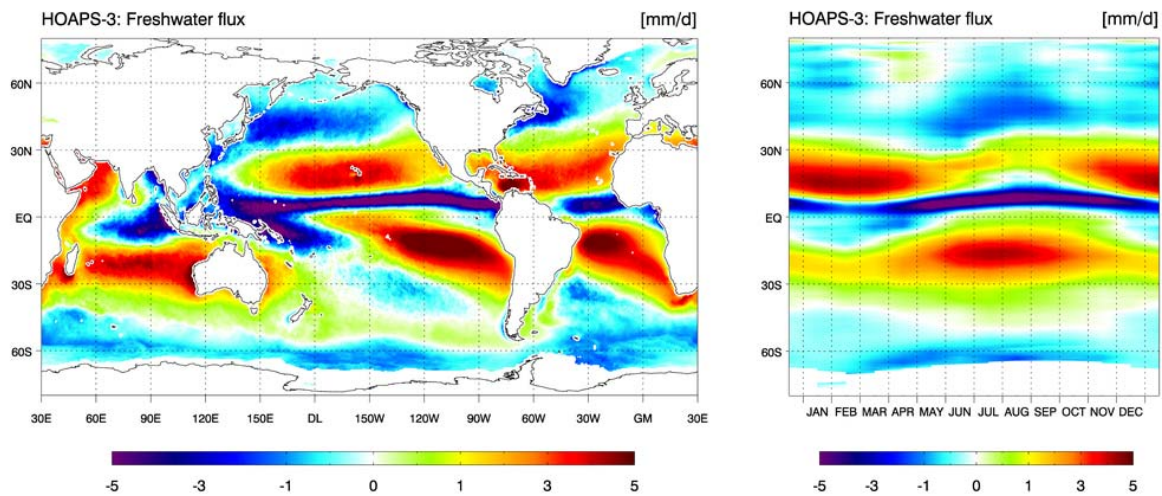


Figure 9: Climatological mean field (left) and zonal mean annual cycle (right) of HOAPS freshwater flux for the years 1988–2005

ocean is mainly found in regions of precipitation maxima in the ITCZ, the midlatitude storm tracks, and at high latitudes. In contrast, subtropical regions generate the major part of the freshwater flux into the atmosphere. In the annual cycle, the dominant features of the input parameters are reproduced.

The difference map of the climatological mean fields of HOAPS and ERA-Interim (Figure 10, top left) is mostly an inversion of the difference between the precipitation datasets shown in Figure 8. In the inner tropics the atmospheric freshwater deficit of ERA-Interim exceeds HOAPS by up to 2 mm/day, while the deficit in HOAPS is larger in the eastern Pacific ITCZ and around 30° north and south. In the eastern Pacific as well as in the Atlantic the difference in the freshwater flux is mostly determined by the evaporation fields.

The differences between HOAPS and the combination of the IFREMER evaporation and GPCP precipitation are less pronounced in the subtropical regions, except for the warm pool and the ITCZ. In the tropical warm pool region the deviations are dominated by the evaporation pattern, while differences in the ITCZ region are mainly due to the deviations of precipitation. At mid- and high latitudes the positive bias in the GPCP precipitation leads to an enhanced freshwater flux into the ocean of IFREMER–GPCP compared to HOAPS.

Additionally, the difference of the combined IFREMER–GPCP product and ERA-Interim is depicted in the lower-right panel of Figure 10. The general patterns of the difference map are similar to the comparison of HOAPS and ERA-Interim with regionally larger amplitudes. In particular the positive bias in the subtropics is larger, and the differences in the ITCZ region are inverted.

The basic structure of the zonal means from each dataset is comparable, as depicted in the lower-left panel of Figure 10. Nevertheless, especially in the tropical regions distinct differences in the magnitude of the mean freshwater flux are evident. South of the equator the positive values of the satellite-derived products indicate a net freshwater flux into the atmosphere, while ERA-Interim shows negative values. This enhanced loss of freshwater from the atmosphere into the ocean in ERA-Interim leads to global monthly mean values that are generally about 0.2 mm/day lower compared to HOAPS and IFREMER–GPCP. The mean globally averaged HOAPS net ocean surface freshwater flux into the atmosphere for the

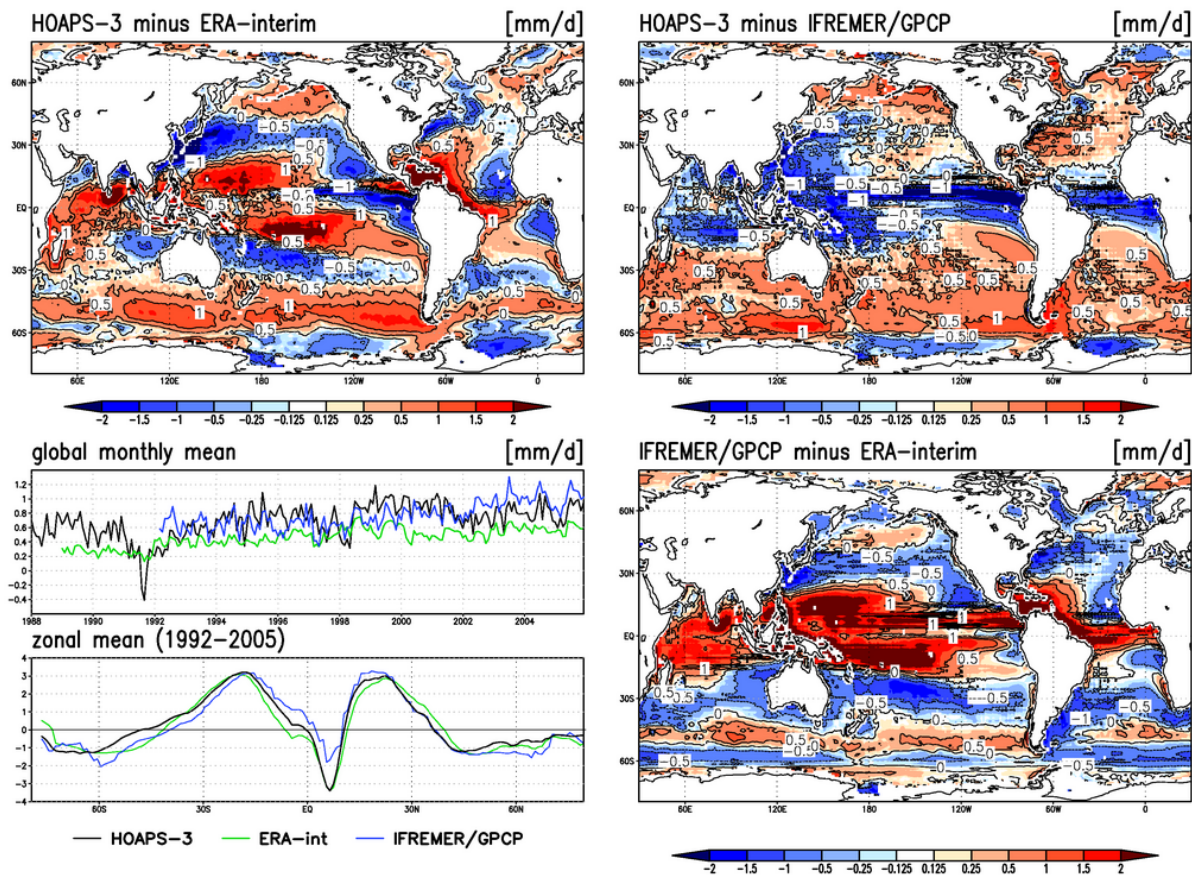


Figure 10: Difference of the 1992–2005 climate mean HOAPS freshwater flux and (upper left) ERA-Interim, (upper right) IFREMER–GPCP, and (lower right) IFREMER–GPCP minus ERA-Interim. The lower-left panel shows the global monthly mean freshwater flux time series of each dataset and the zonal mean freshwater for the overlapping time period 1992–2005.

1992–2005 period is 0.73 mm/day (IFREMER–GPCP: 0.77 mm/day, ERA-Interim: 0.50 mm/day). Furthermore, the time series of both satellite-based datasets exhibit a larger variability with a standard deviation of 0.19 mm/day compared to 0.10 mm/day for ERA-Interim reanalysis data.



5.6.1 Discussion

The mean oceanic freshwater flux in HOAPS for the 1992–2005 period is 0.73 mm/day, which is equivalent to a liquid water volume of about 90,000 km³/a. For a closure of the

Table 5: Requirements for freshwater flux product CM-146 as given in the PRD [RD 1].

Accuracy numbers are given for global mean values. Regional larger deviations may occur.

	Threshold	Target	Optimal
Bias	1.6 mm/d	0.25 mm/d	0.1 mm/d
RMS	2.3 mm/d	0.5 mm/d	0.2 mm/d
Decadal stability	0.13 mm/d	0.015 mm/d	0.002 mm/d

 	EUMETSAT SAF on CLIMATE MONITORING Validation Report HOAPS release 3.2	Doc.No.:SAF/CM/DWD/VAL/HOAPS Issue: 1.1 Date: 25.03.2011
---	---	--

global freshwater balance, this transport of freshwater from the ocean into the atmosphere should be compensated for the most part by continental runoff. Long-term mean runoff data published and summarized by the Global Runoff Data Center (GRDC) add up to a mean value of approximately 0.32 mm/day (equivalent 40,000 km³/a) (GRDC 2009). The uncertainties of different runoff estimates are still in the order of 10%–20%. Additionally, other runoff sources, such as annual ice melt and groundwater flow into the ocean are estimated to be less than 10% of the river discharge (Burnett et al. 2001). Comparing these values to the HOAPS global ocean freshwater flux leaves an imbalance of about 0.4 mm/day in the global freshwater balance. For the combined IFREMER/GPCP fields the imbalance is even larger with nearly 0.5 mm/day. Also for ERA-Interim an imbalance of about 0.2 mm/day remains.

Because of the lack of reliable in situ measurements, the validation of HOAPS monthly mean freshwater flux is done against a combination of other satellite based climatologies and reanalysis data. Comparing HOAPS freshwater flux against the satellite products, it can be concluded that the target requirements defined in the product requirement document are met. (Table 4, PRD [RD 1]). The mean RMS value between HOAPS and the other compared products is 0.2 mm/d.

6 Decadal stability

In order to assess the decadal stability of the HOAPS surface freshwater flux parameters the time-series of global monthly mean anomalies to a reference data set have been analyzed. The reference for each parameter are as defined below:

near surface wind speed	⇒	NOCS
atmospheric humidity	⇒	NOCS
evaporation/latent heat flux	⇒	NOCS
precipitation	⇒	GPCP
freshwater flux	⇒	NOCS – GPCP

Table 6: Results from the decadal stability analysis of global monthly mean anomalies (number are per decade).

Parameter	Decadal stability (CDOP2)		Decadal stability
	Threshold	Target	HOAPS v3.2
Near surface humidity CM-141	1 %	0.5 %	-0.1 %
Near surface wind speed CM-142	0.1 m/s	0.2 m/s	0.09 m/s
Evaporation CM-145	0.1 mm/d	0.015 mm/d	0.09 mm/d
Latent heat flux CM-143	3 W/m ²	0.8 W/m ²	2.7 W/m ²
Precipitation CM-144	0.03 mm/d	0.015 mm/d	-0.01 mm/d
Freshwater flux CM-146	0.13 mm/d	0.015 mm/d	0.1 mm/d

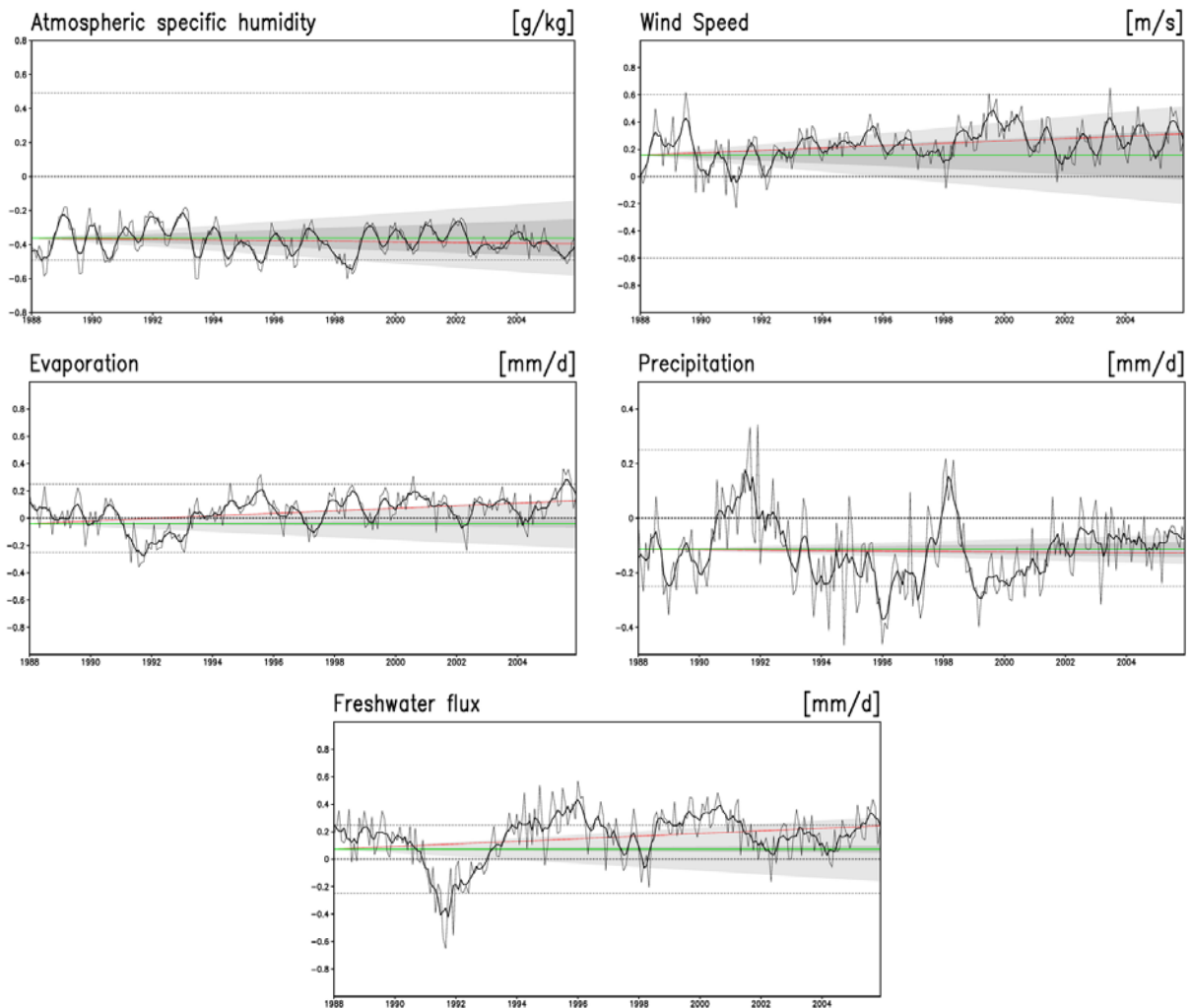



Figure 11: Time series of global monthly mean anomalies of HOAPS parameters minus reference (thin black line) for the time period 1988-2005. The thick black lines are 5-monthly running means. The light grey (dark grey) shaded areas represent the threshold (target). The dotted lines are the target bias requirements for the global mean values. The red line shows the estimated linear trend and the green line is the no-trend line.

Figure 11 shows the anomalies for the overlapping time period from January 1988 to December 2005. As it has been discussed previously, the average global mean values are within the target bias requirement (dotted lines) or better. Table 6 summarizes the results of the linear trend analysis. Anomalies of near-surface humidity and precipitation do not exhibit a significant trend within the overlapping time period. The anomaly of near-surface wind speed is significantly increasing which in turn leads to an increase in evaporation and the freshwater flux. Although these trends are statistically significant they are still within the threshold requirements.

	EUMETSAT SAF on CLIMATE MONITORING Validation Report HOAPS release 3.2	Doc.No.:SAF/CM/DWD/VAL/HOAPS Issue: 1.1 Date: 25.03.2011
---	---	--

7 Conclusions



The HOAPS ocean surface freshwater flux parameters have been compared with evaporation products from ERA-Interim, NOCS v2.0, and IFREMER as well as precipitation fields from ERA-Interim, GPCP, and TRMM. The results show that the different estimates of evaporation and freshwater flux strongly depend on the individual input parameters.

While the general patterns are reproduced by all datasets and global mean time series often agree within a range of 10% of the individual products, locally significant larger deviations occur for all parameters. The satellite-derived datasets often agree better with HOAPS than ERA-Interim and NOCS. However, the compared satellite datasets are not fully independent, as the satellite input data may be of the same origin and/or similar algorithms or parameterizations are used in retrieval procedures. This also accounts to some extent for ERA-Interim, which assimilates a wide range of satellite data.

For the evaporation fields, IFREMER and HOAPS agree well at mid- and high latitudes and most of the tropical regions. Larger differences between both datasets are found over the tropical warm pool region. Here the additional use of scatterometer wind speed data is a disadvantage in the IFREMER dataset, since the used wind speed retrieval is strongly affected by precipitation and introduces errors in the IFREMER evaporation product. This effect is substantially weaker in the HOAPS wind fields, which are derived using only SSM/I data. Here the resulting evaporation fields agree better with ERA-Interim and NOCS. However, in the subtropical regions, the comparisons to ERA-Interim and in particular to the ship-based NOCS data indicate a systematic underestimation of q_{air} by the satellite retrieval used in both HOAPS and IFREMER. The strongest effect of this dry bias in q_{air} is found over the central Pacific, where the difference between HOAPS and NOCS average evaporation values exceeds 1.5 mm/day or 20% in some regions. In the eastern tropical Pacific and Atlantic an inverse effect is evident because of a high bias in the HOAPS q_{air} fields. In the comparison of HOAPS and ERA-Interim evaporation fields the regional biases appear generally lower, but similar patterns as in the comparison with NOCS appear. At mid- and high latitudes the results for the NOCS dataset regionally depend on the data density of the available ship observations. In particular at high latitudes of the Southern Hemisphere the NOCS data exhibit systematic differences compared to the other datasets. In regions with good data sampling the biases between HOAPS and NOCS are significantly lower.

The most potential for improvement of the evaporation parameter appears to be in the humidity (q_{air}) retrievals. The comparisons show an improvement in the biases between the individual q_{air} estimates with respect to previous studies by Chou et al. (2004) and Brunke et al. (2002). But particularly in the tropical regions the resulting evaporation difference patterns are still strongly determined by the deviations in the q_{air} fields. More detailed validation efforts are needed to specify the biases against independent in situ data. Recent results using satellite data of the Advanced Microwave Sounding Unit-A (AMSU-A) indicate that the inclusion of the SST as an additional predictor could improve the q_{air} retrieval (Jackson et al. 2009). Further detailed regional analysis of all parameters required to derive the evaporation AU6 product is envisaged within the SEAFLUX Project of the World Climate Research Programme (WCRP) Global Energy and Water Experiment (GEWEX) Radiation Panel.

In regions with high aerosol load or persistent cloudiness, deficiencies in the SST datasets can cause biases in the q_{sea} fields, affecting the sea–air humidity difference of all products. For example, a low bias in the Pathfinder AVHRR SST of the eastern and central tropical Atlantic due to desert aerosols causes an underestimation of q_{sea} and thus of the evaporation in



 	EUMETSAT SAF on CLIMATE MONITORING Validation Report HOAPS release 3.2	Doc.No.:SAF/CM/DWD/VAL/HOAPS Issue: 1.1 Date: 25.03.2011
---	---	--

HOAPS. Along the African west coast this effects coincides with an overestimation of q_{air} in HOAPS, which enhances the low bias in evaporation. Another unresolved issue is the eruption of Mount Pinatubo in June 1991, which caused large uncertainties in the SST retrievals and hence the flux estimates in the following months.

The precipitation fields of all compared datasets exhibit large differences in highly variable regimes. While the ERA-Interim reanalysis appears to be generally high biased in the tropics, a judgment on the differences between the satellite-based retrievals is difficult because of the lack of extensive and reliable in situ precipitation data. Except for the ITCZ regions, the relative differences in the precipitation bands of the tropical regions are mostly below 20%, while the differences for the extratropical regions are found to be much larger, exceeding 50% regionally. HOAPS is known to perform better than other comparable satellite retrievals at mid and high latitudes (Klepp et al. 2010), where the mixed SSM/I and TOVS retrieval from GPCP exhibits a systematic high bias. Global and regional aspects of precipitation validation are carried out and are planned within the framework of the International Precipitation Working Group (IPWG) and the Program to Evaluate High Resolution Precipitation Products (PEHRPP; <http://essic.umd.edu/msapiano/PEHRPP/>). Encouraging results on quantitative validation efforts of HOAPS regarding frozen precipitation over the cold season Nordic seas motivated further ship campaigns in the near future. Additional in situ validation measurements are foreseen for transects of the tropical ITCZ and the Southern Ocean.


The resulting freshwater flux estimates exhibit distinct differences in terms of global averages as well as regional biases. In the tropical regions, the differences in the precipitation estimates mostly determine the freshwater flux difference patterns. The agreement between the HOAPS and combined IFREMER–GPCP freshwater flux fields is generally better than the agreement of both of them with ERA-Interim. However, compared to long-term mean global river runoff data of about 0.32 mm/day, and even considering their relatively large uncertainties, the ocean surface freshwater balance is not closed by any of the products compared in this study. Since the freshwater flux is the residual of two relatively large values of precipitation and evaporation, a closure of the global balance without constraints from the respective continental values is extremely difficult. With an average value of 0.5 mm/day for E - P, the remaining imbalance of 0.2 mm/day for ERA-Interim is smaller than the satellite-based estimates, but the spatial distribution of the freshwater flux field appears to be questionable in the tropical regions because of the excessive precipitation. For HOAPS the global ocean freshwater balance is closed within a range of 10%–15% (0.4 mm/day) of the individual global mean evaporation and precipitation estimates. For the combined IFREMER–GPCP fields the imbalance is slightly larger (0.5 mm/day).

Based on the comparisons presented in this report, we conclude that the HOAPS dataset is within target accuracies or better and provides consistent fields of evaporation, precipitation, and the resulting freshwater flux that are well suited for further studies of the freshwater flux and related parameters on climatological and regional scale. Overall, the imbalance in the global ocean surface freshwater flux is greatly reduced compared to previous versions of HOAPS because of the new precipitation algorithm introduced in HOAPS-3. Notwithstanding the remaining imbalance, the variability of the freshwater flux parameters with respect to climate indices such as the North Atlantic Oscillation is well represented in HOAPS-3, as shown by Andersson et al. (2010a). However, more detailed validation efforts are needed to explain and, if possible, remove the remaining biases between the different datasets.


 	EUMETSAT SAF on CLIMATE MONITORING Validation Report HOAPS release 3.2	Doc.No.:SAF/CM/DWD/VAL/HOAPS Issue: 1.1 Date: 25.03.2011
---	---	--

8 References


- Adler, R. F., C. Kidd, G. Petty, M. Morissey, and H. Goodman, 2001: Intercomparison of global precipitation products: The third Precipitation Intercomparison Project (PIP-3). *Bull. Amer. Meteor. Soc.*, 82, 1377–1396.
- , and Coauthors, 2003: The Version-2 Global Precipitation Climatology Project (GPCP) monthly precipitation analysis (1979–present). *J. Hydrometeor.*, 4, 1147–1167.
- Allan, R. P., and B. G. Liepert, 2010: Anticipated changes in the global atmospheric water cycle. *Environ. Res. Lett.*, 5, 025201, doi:10.1088/1748-9326/5/2/025201.
- Andersson, A., S. Bakan, K. Fennig, H. Graßl, C. Klepp, and J. Schulz, cited 2007: Hamburg Ocean Atmosphere Parameters and Fluxes from Satellite Data—HOAPS-3—Monthly mean. World Data Center for Climate. [Available online at http://cerawww.dkrz.de/WDCC/ui/Compact.jsp?acronym5HOAPS3_MONTHLY.]
- , ———, and H. Graßl, 2010a: Satellite derived precipitation and freshwater flux variability and its dependence on the North Atlantic Oscillation. *Tellus*, 62, 453–468.
- , K. Fennig, C. Klepp, S. Bakan, H. Graßl, and J. Schulz, 2010b: The Hamburg Ocean Atmosphere Parameters and Fluxes from Satellite Data—HOAPS-3. *Earth Syst. Sci. Data*, 2, 215–234, doi:10.5194/essd-2-215-2010, 2010.
- Bentamy, A., K. B. Katsaros, A.M.Mestas-Nunez, W.M. Drennan, E. B. Forde, and H. Roquet, 2003: Satellite estimates of wind speed and latent heat flux over the global oceans. *J. Climate*, 16, 637–656.
- , L. H. Ayina, W. Drennan, K. Katsaros, A. M. Mestas-Nunez, and R. T. Pinker, 2008: 15 years of ocean surface momentum and heat fluxes from remotely sensed observations. *FLUXNEWS*, Vol. 5, WCRP Working Group on Surface Fluxes, World Climate Research Programme, Geneva, Switzerland, 14–16.
[Available online at http://sail.msk.ru/newsletter/fluxnews_5_final.pdf.]
- Beranger, K., B. Barnier, S. Gulev, and M. Crepon, 2006: Comparing 20 years of precipitation estimates from different sources over the world ocean. *Ocean Dyn.*, 56, 104–138.
- Berry, D. I., and E. C. Kent, 2009: A new air–sea interaction gridded dataset from ICOADS with uncertainty estimates. *Bull. Amer. Meteor. Soc.*, 90, 645–656.
- Bourras, D., L. Eymard, and W. T. Liu, 2002: A neural network to estimate the latent heat flux over oceans from satellite observations. *Int. J. Remote Sens.*, 23, 2405–2423.
- Bourras, D., 2006: Comparison of five satellite-derived latent heat flux products to moored buoy data. *J. Climate*, 19, 6291–6313.
- Bowman, K. P., C. R. Homeyer, and D. G. Stone, 2009: A comparison of oceanic precipitation estimates in the tropics and subtropics. *J. Appl. Meteor. Climatol.*, 48, 1335–1344.
- Brunke, M. A., X. Zeng, and S. Anderson, 2002: Uncertainties in sea surface turbulent flux algorithms and data sets. *J. Geophys. Res.*, 107, 3141, doi:10.1029/2001JC000992.
- Burnett, W. C., M. Taniguchi, and J. Oberdorfer, 2001: Measurement and significance of the direct discharge of groundwater into the coastal zone. *J. Sea Res.*, 46, 109–116.
- Casey, K. S., 2004: Global AVHRR 4 km SST for 1985–2001, Pathfinder V5.0, NODC/RSMAS. Tech. Rep., NOAA National Oceanographic Data Center

	EUMETSAT SAF on CLIMATE MONITORING Validation Report HOAPS release 3.2	Doc.No.:SAF/CM/DWD/VAL/HOAPS Issue: 1.1 Date: 25.03.2011
---	---	--



- Chou, S. H., E. Nelkin, J. Ardizzone, R. M. Atlas, and C. L. Shie, 2003: Surface turbulent heat and momentum fluxes over global oceans based on the Goddard satellite retrievals, version 2 (GSSTF2). *J. Climate*, 16, 3256–3273.
- , ———, ———, and ———, 2004: A comparison of latent heat fluxes over global oceans for four flux products. *J. Climate*, 17, 3973–3989.
- Fairall, C. W., E. F. Bradley, D. P. Rogers, J. B. Edson, and G. S. Young, 1996: Bulk parameterization of air–sea fluxes for Tropical Ocean–Global Atmosphere Coupled Ocean–Atmosphere Response Experiment. *J. Geophys. Res.*, 101, 3747–3764.
- , ———, J. E. Hare, A. A. Grachev, and J. B. Edson, 2003: Bulk parameterization of air–sea fluxes: Updates and verification for the COARE algorithm. *J. Climate*, 16, 571–591.
- GRDC, cited 2009: Surface freshwater fluxes into the world oceans/Global Runoff Data Centre: Comparisons of GRDC freshwater flux estimate with literature. Federal Institute of Hydrology (BfG), Koblenz, Germany. [Available online at http://www.bafg.de/cln_007/nn_317460/sid_F743821E9F88AD083AD1C494E3D95FDE/nsc_true/GRDC/EN/02__Services/02__DataProducts/FreshwaterFluxes/freshflux__node.html?__nnn5true.]
- GSFC, cited 2007: Algorithm 3B43—TRMM and other data precipitation. Goddard Space Flight Center. [Available online at <http://trmm.gsfc.nasa.gov/3b43.html>.]
- Hilburn, K. A., and F. J. Wentz, 2008: Intercalibrated passive microwave rain products from the Unified Microwave Ocean Retrieval Algorithm (UMORA). *J. Appl. Meteor. Climatol.*, 47, 778–794.
- Hsu, K., X. Gao, S. Sorooshian, and H. Gupta, 1997: Precipitation estimation from remotely sensed information using artificial neural networks. *J. Appl. Meteor.*, 36, 1176–1190.
- Huffman, G. J., and Coauthors, 1997: The Global Precipitation Climatology Project (GPCP) combined precipitation dataset. *Bull. Amer. Meteor. Soc.*, 78, 5–20.
- , and Coauthors, 2007: The TRMM Multisatellite Precipitation Analysis (TMPA): Quasi-global, multiyear, combined-sensor precipitation estimates at fine scales. *J. Hydrometeorol.*, 8, 38–55.
- Jackson, D. L., G. A. Wick, and F. R. Robertson, 2009: Improved multisensor approach to satellite-retrieved near-surface specific humidity observations. *J. Geophys. Res.*, 114, D16303, doi:10.1029/2008JD011341.
- Janowiak, J. E., A. Gruber, C. R. Kondragunta, R. E. Livezey, and G. J. Huffman, 1998: A comparison of the NCEP–NCAR reanalysis precipitation and the GPCP rain gauge–satellite combined dataset with observational error considerations. *J. Climate*, 11, 2960–2979.
- Jones, C., P. Peterson, and C. Gautier, 1999: A new method for deriving ocean surface specific humidity and air temperature: An artificial neural network approach. *J. Appl. Meteor.*, 38, 1229–1246.
- Kalnay, E., and Coauthors, 1996: The NCEP/NCAR 40-Year Reanalysis Project. *Bull. Amer. Meteor. Soc.*, 77, 437–471. Kanamitsu, M., W. Ebisuzaki, J. Woollen, S.-K. Yang, J. J. Hnilo,
- M. Fiorino, and G. L. Potter, 2002: NCEP–DOE AMIP-II Reanalysis (R-2). *Bull. Amer. Meteor. Soc.*, 83, 1631–1643.

	EUMETSAT SAF on CLIMATE MONITORING Validation Report HOAPS release 3.2	Doc.No.:SAF/CM/DWD/VAL/HOAPS Issue: 1.1 Date: 25.03.2011
---	---	--

- Kelly, K. A., S. Dickinson, M. J. McPhaden, and G. C. Johnson, 2001: Ocean currents evident in satellite wind data. *Geophys. Res. Lett.*, 28, 2469–2472.
- Klepp, C. P., S. Bakan, and H. Graßl, 2003: Improvements of satellite-derived cyclonic rainfall over the North Atlantic. *J. Climate*, 16, 657–669.
- , ———, and ———, 2005: Missing North Atlantic cyclonic precipitation in ECMWF numerical weather prediction and ERA-40 data detected through the satellite climatology HOAPS II. *Meteor. Z.*, 14, 809–821.
- Klepp, C., K. Bumke, S. Bakan, and P. Bauer, 2010: Ground validation of oceanic snowfall detection in satellite climatologies during LOFZY. *Tellus*, 62, 469–480.
- Kubota, M., N. Iwasaka, S. Kizu, M. Kondo, and K. Kutsuwada, 2002: Japanese ocean flux data sets with use of remote sensing observations (J-OFURO). *J. Oceanogr.*, 58, 213–225.
- Kubota, M., and H. Tomita, 2007: Introduction of J-OFURO latent heat flux version 2. *Proc. Joint 2007 EUMETSAT Meteorological Satellite Conf. and 15th Satellite Meteorology and Oceanography Conf.*, Amsterdam, Netherlands, EUMETSAT and Amer. Meteor. Soc.
- Kubota, T., and Coauthors, 2007: Global precipitation map using satellite-borne microwave radiometers by the GSMaP project: Production and validation. *IEEE Trans. Geosci. Remote Sens.*, 45, 2259–2275.
- Liu, J. P., and J. A. Curry, 2006: Variability of the tropical and subtropical ocean surface latent heat flux during 1989–2000. *Geophys. Res. Lett.*, 33, L05706, doi:10.1029/2005GL024809.
- Liu, W., A. Zhang, and J. Bishop, 1994: Evaporation and solar irradiance as regulators of sea surface temperature in annual and interannual changes. *J. Geophys. Res.*, 99 (C6), 12 623–12 638.
- Meissner, T., D. Smith, and F. Wentz, 2001: A 10 year intercomparison between collocated Special Sensor Microwave Imager oceanic surface wind speed retrievals and global analyses. *J. Geophys. Res.*, 106, 11 731–11 742.
- Monahan, A. H., 2006: The probability distribution of sea surface wind speeds. Part II: Dataset intercomparison and seasonal variability. *J. Climate*, 19, 521–534.
- Murray, F. W., 1967: On the computation of saturation vapour pressure. *J. Appl. Meteor.*, 6, 203–204.
- NODC, cited 2008: 4 km Pathfinder Version 5 User Guide. Silver Spring, Maryland, National Oceanographic Data Center. [Available online at <http://www.nodc.noaa.gov/sog/pathfinder4km/userguide.html>.]
- Onogi, K., and Coauthors, 2007: The JRA-25 Reanalysis. *J. Meteor. Soc. Japan*, 85, 369–432.
- Sapiano, M. R. P., and P. A. Arkin, 2009: An intercomparison and validation of high-resolution satellite precipitation estimates with 3-hourly gauge data. *J. Hydrometeorol.*, 10, 149–166.
- Schlosser, C. A., and P. R. Houser, 2007: Assessing a satellite-era perspective of the global water cycle. *J. Climate*, 20, 1316–1338.

	EUMETSAT SAF on CLIMATE MONITORING Validation Report HOAPS release 3.2	Doc.No.:SAF/CM/DWD/VAL/HOAPS Issue: 1.1 Date: 25.03.2011
---	---	--

- Schulz, J., P. Schluessel, and H. Graßl, 1993: Water-vapor in the atmospheric boundary layer over oceans from SSM/I measurements. *Int. J. Remote Sens.*, 14, 2773–2789.
- Shinoda, T., H. H. Hendon, and J. Glick, 1999: Intraseasonal surface fluxes in the tropical western pacific and Indian oceans from NCEP reanalyses. *Mon. Wea. Rev.*, 127, 678–693.
- Simmons, A., S. Uppala, D. Dee, and S. Kobayashi, 2007: ERA– Interim: New ECMWF reanalysis products from 1989 onwards. *ECMWF Newsletter*, No. 110, ECMWF, Reading, United Kingdom, 25–35.
- Smith, S. D., 1980: Wind stress and heat flux over the ocean in gale force winds. *J. Phys. Oceanogr.*, 10, 709–726.
- , 1988: Coefficients for sea surface wind stress, heat flux, and wind profiles as a function of wind speed and temperature. *J. Geophys. Res.*, 93 (C12), 15 467–15 472.
- Swift, C. T., L. S. Fedor, and R. O. Ramseier, 1985: An algorithm to measure sea ice concentration with microwave radiometers. *J. Geophys. Res.*, 90, 1087–1099.
- Tournadre, J., and Y. Quilfen, 2003: Impact of rain cell on scatterometer data: 1. Theory and modeling. *J. Geophys. Res.*, 108, 3225, doi:10.1029/2002JC001428.
- Trenberth, K. E., and C. J. Guillemot, 1998: Evaluation of the atmospheric moisture and hydrological cycle in the NCEP/NCAR reanalyses. *Climate Dyn.*, 14, 213–231.
- , L. Smith, T. Qian, A. Dai, and J. Fasullo, 2007: Estimates of the global water budget and its annual cycle using observational and model data. *J. Hydrometeor.*, 8, 758–769.
- , J. T. Fasullo, and J. Kiehl, 2009: Earth’s global energy budget. *Bull. Amer. Meteor. Soc.*, 90, 311–323.
- Uppala, S. M., and Coauthors, 2005: The ERA-40 Re-Analysis. *Quart. J. Roy. Meteor. Soc.*, 131, 2961–3012.
- Wallcraft, A., A. Kara, C. Barron, E. Metzger, R. Pauley, and M. Bourassa, 2009: Comparisons of monthly mean 10 m wind speeds from satellites and NWP products over the global ocean. *J. Geophys. Res.*, 114, D16109, doi:10.1029/2008JD011696.
- Wentz, F. J., 1997: A well-calibrated ocean algorithm for Special Sensor Microwave/Imager. *J. Geophys. Res.*, 102 (C4), 8703–8718.
- , L. Ricciardulli, K. Hilburn, and C. Mears, 2007: How much more rain will global warming bring? *Science*, 317, 233–235.
- Winterfeldt, J., A. Andersson, C. Klepp, S. Bakan, and R. Weisse, 2010: Comparison of HOAPS, QuikSCAT and buoy wind speed in the eastern North Atlantic and the North Sea. *IEEE Trans. Geosci. Remote Sens.*, 48, 338–348.
- Worley, S., S. Woodruff, R. Reynolds, S. Lubker, and N. Lott, 2005: ICOADS release 2.1 data and products. *Int. J. Climatol.*, 25, 823–842.
- Xie, P., and P. Arkin, 1997: Global precipitation: A 17-year monthly analysis based on gauge observations, satellite estimates, and numerical model outputs. *Bull. Amer. Meteor. Soc.*, 78, 2539–2558.
- Yu, L. S., and R. A. Weller, 2007: Objectively analyzed air–sea heat fluxes for the global ice-free oceans (1981–2005). *Bull. Amer. Meteor. Soc.*, 88, 527–539.

 	EUMETSAT SAF on CLIMATE MONITORING Validation Report HOAPS release 3.2	Doc.No.:SAF/CM/DWD/VAL/HOAPS Issue: 1.1 Date: 25.03.2011
---	---	--

—, X. Jin, and R. A. Weller, 2008: Multidecade global flux datasets from the objectively analyzed air–sea fluxes (OAFlux) project: Latent and sensible heat fluxes, ocean evaporation, and related surface meteorological variables. Tech. Rep. OA- 2008-01, Woods Hole Oceanographic Institution, OAFlux Project, 64 pp.